NASA TECHNICAL NOTE

NASA TN D-3950

NASA TN D-3950

SINGLE-PHASE INDUCTION ELECTROMAGNETIC PUMP

by Richard E. Schwirian

Lewis Research Center

Cleveland, Ohio

NATIONAL AERONAUTICS AND SPACE ADMINISTRATION • WASHINGTON, D. C. • MAY 1967

NASA TN D-3950

SINGLE-PHASE INDUCTION ELECTROMAGNETIC PUMP

By Richard E. Schwirian

Lewis Research Center
Cleveland, Ohio

NATIONAL AERONAUTICS AND SPACE ADMINISTRATION

For sale by the Clearinghouse for Federal Scientific and Technical Information
Springfield, Virginia 22151 – CFSTI price $3.00

SINGLE-PHASE INDUCTION ELECTROMAGNETIC PUMP

by Richard E. Schwirian

Lewis Research Center

SUMMARY

Analyses of two single-phase induction electromagnetic pumps in which induced electrical currents flow circumferentially in an annulus are presented. The analysis assumes a purely radial magnetic field, and differential equations describing the dependence of the magnetic field on the axial coordinate are obtained by using the integrated form of Ampere's law, Maxwell's equations, and Ohm's law. General solutions to these equations are obtained and are applied to specific configurations by assigning the appropriate boundary conditions at the annulus inlet and outlet.

Performance of single-phase induction pumps is largely dependent on two dimensionless quantities, flow magnetic Reynolds number and frequency magnetic Reynolds number. Dimensionless functions of these magnetic Reynolds numbers are developed from which calculations of developed pressure, efficiency, core magnetic field strength, and current-voltage requirements can be made. Calculations of efficiency and dimensionless developed pressure are also made. It is shown that, for the cases of low flow magnetic Reynolds number with low frequency magnetic Reynolds number and high flow magnetic Reynolds number with low frequency magnetic Reynolds number, simple expressions for ideal efficiency can be obtained.

Finally, a comparison of these single-phase induction pump designs with traveling-field induction pumps of similar geometry is made. For the particular application considered, the efficiency differences between single-phase and traveling-field pumps are negligible. Furthermore, single-phase pumps are potentially more reliable than traveling-field pumps at high temperatures and are, therefore, more adaptable to space power systems.

INTRODUCTION

In space electric power systems using the liquid alkali metals either as a working fluid or as a heat-transfer medium, a need exists for pumping units of high reliability,

low weight, and high efficiency. For such systems, both the impeller-type pump and the electromagnetic pump are being considered.

To date, attention has been focused primarily on the canned motor-driven impeller pump for space application because of its somewhat higher predicted efficiency and lower predicted weight as compared with conventional electromagnetic pumps. Recent studies (ref. 1), however, indicate that, for space applications, electromagnetic pumping systems having weights comparable to motor-driven impeller pumping systems can be designed. Furthermore, the reliability gained by eliminating the necessity of bearings and seals and all other moving parts makes the electromagnetic pump quite attractive.

The most potentially reliable of all electromagnetic pumps for application in high-temperature space power systems is the single-phase induction pump. Induction electromagnetic pumps generally are more reliable than conduction electromagnetic pumps because of the lack of electrodes, thereby eliminating the mechanically difficult electrode-duct connections. As opposed to the only other induction pump (the traveling-field device), the single-phase pump has an advantage in that the exciting coils need not be placed in close proximity to the hot fluid. Coil electrical insulation problems are therefore simplified, and coil electrical losses are decreased because of the reduced coil temperature. Because of this advantage, the single-phase pump should be more adaptable to high-temperature applications than conduction or traveling-field pumps.

Disadvantages of the single-phase pump are its low ideal efficiency, high weight, and the unsteady nature of the developed pressure (see ref. 1). Even though the maximum obtainable ideal efficiency of single-phase pumps is less than the maximum obtainable ideal efficiency of traveling-field pumps, real efficiencies could be comparable or greater. The reasons for this are twofold: First, lower coil losses are made possible by a lower coil temperature. Second, for a required number of excitation ampere turns, the coil losses can be further reduced by increasing the coil size and, therefore, decreasing the current density. This is done, however, at the expense of increased pump weight.

The single-phase pump was first conceived by Watt (ref. 2). In his report, Watt considered the magnetic-field distortion created when an alternating, transverse magnetic field is impressed on a conducting fluid flowing axially in an annular duct. Appropriate boundary conditions are applied and curves of magnetic field strength against axial distance are presented. Rhudy (ref. 1) extended Watt's work to include approximate corrections for the effects of nonzero duct-wall conductivity and also presented equations that could be used for computing output pressure and both fluid and duct-wall electrical losses. Rhudy also suggested another single-phase pump configuration that required less magnetic material than Watt's configuration but was less efficient. In neither of these papers were general performance characteristics of single-phase pumps discussed or general curves of performance presented.

The purpose of this report is to make an analysis of two single-phase induction pumps and to obtain general performance curves from which the parameters that will optimize the performance of such pumps can be determined. Performance is shown to depend largely on the two dimensionless quantities, flow magnetic Reynolds number and frequency magnetic Reynolds number, where magnetic Reynolds number is defined as the dimensionless product of a characteristic permeability, electrical conductivity, velocity, and length of the system. Curves of ideal efficiency, dimensionless ideal pressure, and dimensionless core magnetic field strength are given as functions of these two magnetic Reynolds numbers for two types of the single-phase pump. Other dimensionless functions that can be used to compute nonideal performance and current-voltage requirements are also presented, and trends at low values of flow and frequency magnetic Reynolds numbers are discussed. Finally, comparisons of performance with that of annular traveling-field pump, which is geometrically quite similar to the single-phase pump under consideration, are made, and conclusions are reached concerning efficiency, reliability, and weight.

ANALYSIS

Single-Phase Pump Concept

The body force in many electromagnetic pumps, including the single-phase pump, can be considered as resulting from a magnetic pressure gradient. This concept will be quite convenient in understanding single-phase pump operation.

The equations governing the distribution and magnitude of the electric and magnetic fields $\vec{E}$ and $\vec{B}$ in an isotropic, charge-free medium, are, when displacement current terms are neglected,

$$\nabla \times \vec{E} = -\frac{\partial \vec{B}}{\partial t} \qquad \text{(Faraday's law)} \tag{1}$$

$$\nabla \times \vec{B} = \mu \vec{j} \qquad \text{(Ampere's law)} \tag{2}$$

$$\nabla \cdot \vec{B} = 0 \tag{3}$$

$$\nabla \cdot \vec{E} = 0 \tag{4}$$

$$\vec{j} = \sigma\left(\vec{E} + \vec{v} \times \vec{B}\right) \qquad \text{(Ohm's law)} \tag{5}$$

(Symbols are defined in appendix A.)

For any system to which the aforementioned assumptions apply, equations (1) to (5) must be satisfied. If a complete analytical solution for electric field strength $\vec{E}$ and

magnetic field strength $\vec{B}$ is obtainable, then current density $\vec{j}$ can be computed according to Ohm's law (eq. (5)) or Ampere's law (eq. (2)). For conduction and traveling-field electromagnetic pumps, electrical current can conveniently be thought of as arising from the presence, in a medium of electrical conductivity σ, of a field $\vec{E} + \vec{v} \times \vec{B}$. This point of view is suggested by Ohm's law. A less common but equally valid point of view is to consider electrical current as a manifestation of a distorted magnetic field. This latter point of view is most helpful in understanding the principle of operation of the single-phase induction pump.

Consider the situation depicted in figure 1(b) in which a conducting fluid flows with velocity $\vec{v}$ through a magnetic field of finite extent in the z-direction. If the magnetic field strength $\vec{B}$ is assumed to have a component in the y-direction only and if the y- and x-derivatives are neglected, equations (2) and (5) imply that

$$\frac{1}{\mu} \frac{\partial B_y}{\partial z} = \sigma v B_y \tag{6}$$

Solving equation (6) gives

$$B_y = C_0 e^{\mu\sigma v z} \tag{7}$$

If a certain amount of magnetic flux φ_m must pass through the fluid, then the appropriate boundary condition is

$$\varphi_m = \int_0^C C_0 e^{\mu\sigma v z} \, dz \tag{8}$$

for a unit width in x-direction. Equation (8) determines the constant C_0:

$$C_0 = \frac{\mu\sigma v \varphi_m}{e^{\mu\sigma v C} - 1} \tag{9}$$

A plot of magnetic-field strength B_y against z is given in figure 1(a) for a hypothetical case in which $C_0 = 1$ weber per square meter, and the flow magnetic Reynolds number $Re_{mv} = \mu\sigma v C = \ln 2$. The total force exerted on the fluid can be computed by integrating the Lorentz force $\vec{j} \times \vec{B}$ over the volume occupied by the fluid:

$$\text{Total force } \vec{F} = g \int_0^C \left(\vec{j} \times \vec{B} \right) dz \tag{10}$$

for a unit width in the x-direction.

Computing $\vec{j}$ from Ampere's law gives

$$\left.\begin{aligned} \vec{j} &= -\frac{1}{\mu}\frac{\partial B_y}{\partial z}\hat{i} \\ &= -\frac{1}{\mu}\frac{dB_y}{dz}\hat{i} \\ j \times B &= -\frac{1}{\mu} B_y \frac{\partial B_y}{\partial z}\hat{k} \\ &= -\frac{1}{2\mu}\frac{d(B_y)^2}{dz}\hat{k} \end{aligned}\right\} \qquad (11)$$

Therefore,

$$\frac{\vec{F}}{g} = -\frac{\hat{k}}{2\mu}\int_0^C \frac{d(B_y)^2}{dz}\,dz$$

$$= \frac{1}{2\mu}\left[B_y^2(0) - B_y^2(C)\right]\hat{k}$$

= Inlet magnetic pressure - Outlet magnetic pressure

where magnetic pressure is defined as the quantity $B_y^2/2\mu$. Note that, if $B_y^2(0) > B_y^2(C)$, then equation (11) states that $\vec{F}$ is in the positive z-direction; whereas, if $B_y^2(C) > B_y^2(0)$, a retarding force results. The sign of the force, therefore, depends only on the relative magnitudes of $B_y^2(0)$ and $B_y^2(C)$. For the situation depicted in figure 1(a), $B_y^2(C) > B_y^2(0)$ and hence the force is negative. In the traveling-field electromagnetic pump, $B_y^2(0)$ is made greater than $B_y^2(C)$ by forcing the magnetic field to travel with a velocity $\vec{v}_w$ that is in the same direction but has greater velocity than the fluid velocity $\vec{v}$. The relative velocity $\vec{v}_s = \vec{v} - \vec{v}_w$ is therefore negative, and equation (7) becomes

$$B_y = C_0 e^{\mu\sigma v_s z}$$

$$= C_0 e^{-\mu\sigma V_s z} \qquad (12)$$

where $v_s = -V_s$ and V_s is a positive number. Equation (12) shows that $B_y^2(0) > B_y^2(C)$, and a positive force results. For electromagnetic pumps in which current is supplied from an external source (conduction pumps), such a simple description as this is not possible; however, it can be shown that the magnetic pressure difference concept still holds. An example is given in appendix B.

The previous discussion and examples were presented in order to show that the electromagnetic body force can be thought of as the manifestation of an asymmetric magnetic field rather than as the interaction of electric and magnetic fields. The latter, perhaps, has more physical meaning, but the former point of view is more convenient for describing the principle of operation of the single-phase induction pump. The following sections show that the single-phase induction pumping principle results from boundary conditions that cause the average magnetic pressure at pump inlet to be greater than that at pump outlet, resulting in a positive pumping force.

Proposed Model and Assumptions

The systems to be analyzed are pictured in figure 2. In both cases a conducting fluid flows axially in an annulus bounded on either side by a core of high-permeability magnetic material. A radial, time-varying magnetic field, whose strength varies both in time and space, is used to pump the fluid. Coils wound circumferentially around the low-radius portion of the magnetic core near the annulus inlet produce this magnetic field. Inlet and outlet pipes leading to and from the annulus may be either radial or axial depending on which is more convenient.

Hereinafter, the configuration depicted in figure 2(a) will be referred to as type A and the configuration in figure 2(b) as type B. From figure 2 it is apparent that the only difference between the two configurations is that, in the type A pump, a low reluctance path for the magnetic field is provided at the annulus outlet side of the pump.

The assumptions made in the analyses of these two pumps are as follows:

(1) The magnetic field in the annulus has a component in the radial direction only.

(2) The permeability of the magnetic core is much larger than that of free space.

(3) Fringing of the magnetic field at each end of the annulus can be neglected.

(4) All materials of the annulus, including the fluid, are isotropic, nonmagnetic, charge-free, and have a permeability equal to that of free space.

(5) The magnetic field produced by electrical-current flow in the fluid outside the annulus is negligible.

(6) Electrical losses due to current flow in fluid outside the annulus are negligible.

(7) The fluid in the annulus has a velocity component in the axial direction only.

(8) Displacement currents can be neglected.

The first of these assumptions should be valid as long as the annulus length in the axial direction is large as compared with the annulus width in the radial direction. The third assumption should be valid for large values of the ratio of annulus axial length to radial width. For very high values of the appropriate magnetic Reynolds numbers (defined in the next section), however, fringing at the annulus inlet is unavoidable. The results presented in this report are, therefore, limited to "low" magnetic Reynolds numbers. The word "low" here does not necessarily mean less than 1 but is intended merely to indicate that fringing will become significant at some value of the appropriate magnetic Reynolds number. The fifth assumption should be valid if the fluid outside the annulus is not allowed to form a closed circumferential path in which induced current may flow. This stipulation can be accomplished either by using multiple inlet pipes or by placing insulating baffles perpendicular to induced current flow in single inlet and outlet pipes. The sixth assumption is related to the fifth assumption and should also be valid if sufficient baffling, either by multiple pipes or baffles, is provided.

Governing Equations

The analysis to be presented herein will be primarily concerned with determining the magnetic field in the pump annulus. The only consideration of the total magnetic circuit necessary will be that which is essential to determine the appropriate boundary conditions.

For the assumed configuration, a cylindrical coordinate system, as indicated in figure 3, is most convenient. Fluid velocity $\vec{v}$ is given by

$$\vec{v} = v\hat{k} \tag{13}$$

That the magnetic field has a component in the radial direction only has been assumed. Therefore, the magnetic field strength $\vec{B}$ can be written

$$\vec{B} = B_r\hat{r} = B\hat{r} \tag{14}$$

Assuming axial symmetry ($\partial/\partial\theta = 0$) and a sinusoidal dependence of magnetic field strength $\vec{B}$ on time t produces

$$B = \alpha'(r, z)e^{i\omega t} \tag{15}$$

Equation (3) implies that

$$\frac{\partial}{\partial r}(rB) = 0$$

Substituting for B from equation (15) yields the following:

$$e^{i\omega t}\frac{\partial}{\partial r}(r\alpha') = 0 \tag{16}$$

This equation can be satisfied in general only if

$$\frac{\partial}{\partial r}(r\alpha') = 0$$

which implies that

$$\alpha'(r, z) = \frac{\alpha(z)}{r} \tag{17}$$

Faraday's law (eq. (1)), axial symmetry, and equation (4) further require that

$$\frac{\partial}{\partial r}(rE_\theta) = 0 \tag{18}$$

$$\frac{\partial E_\theta}{\partial z} = \frac{\partial B}{\partial t} \tag{19}$$

$$\frac{\partial E_z}{\partial r} = \frac{\partial E_r}{\partial z} \tag{20}$$

$$\frac{\partial E_z}{\partial z} + \frac{1}{r}\frac{\partial}{\partial r}(rE_r) = 0 \tag{21}$$

Assuming also that E_θ is sinusoidal in time yields

$$E_\theta = \gamma'(r, z)e^{i\omega t} \tag{22}$$

Equation (18) then implies

$$\gamma'(r, z) = \frac{\gamma(z)}{r} \tag{23}$$

Equation (19) reduces to

$$\frac{d\gamma}{dz} = i\omega\alpha \tag{24}$$

Equations (20) and (21) suggest writing E_z and E_r as gradients of a potential function. For the case under consideration, however, no potential electric fields are applied, and since current flow in the annulus is uninterrupted by nonconducting dividers, none should arise. Therefore, the appropriate solutions for E_r and E_z are

$$E_r = E_z = 0$$

In order to obtain the magnetic field strength B as a function of the axial coordinate z, Ampere's law, in integrated form, will be required. For the system under consideration, this form is

$$\oint_P \vec{H} \cdot d\vec{l} = \int_A \vec{j} \cdot d\vec{A} \tag{25}$$

Equation (25) states that the line integral of the magnetic intensity $\vec{H}$ around a closed path P is equal to the electrical current flow through the area A enclosed by the path P. For the situation depicted in figure 3, the path P to be considered is the path abcd. The segments ab and cd are taken to be just long enough to enclose all material within the gap. Furthermore, segment ab is taken to be at the annulus inlet so that the magnetic intensity here is a function of radius and time only. Also, since the magnetic core has been assumed to have a permeability much higher than all other media in the annulus, the line integrals of the magnetic intensity $\vec{H}$ over paths bc and da are zero in comparison with the same integrals over paths ab and cd; that is,

$$\int_{bc} \vec{H} \cdot d\vec{l} \cong \int_{da} \vec{H} \cdot d\vec{l} \cong 0$$

Therefore, equation (25) reduces to

$$\int_{cd} \vec{H} \cdot d\vec{l} + \int_{ab} \vec{H} \cdot d\vec{l} = \int_{A_{abcd}} \vec{j} \cdot d\vec{A} \tag{26}$$

Before proceeding further, note that the only assumptions made about the materials in the gap are that they be isotropic, charge-free, and nonmagnetic. Any number of conducting, nonconducting, flowing, or stationary materials is allowable, as long as the assumption of unidirectional magnetic field strength is valid. Figure 3 shows a typical case in which the pumped fluid and a cooling fluid flow in the annulus and are contained by four duct walls. For some situations, thermal insulation and several duct materials may be necessary. In general, assume n materials to be enclosed in the annulus, each with a conductivity σ_k and flowing with an axial speed v_k. From equation (5) it follows that the current density in the k^{th} material is given by

$$\vec{j}_k = \sigma_k(E_\theta + v_k B)\hat{\theta} \tag{27}$$

From substituting equations (15), (17), (22), and (23), equation (27) becomes

$$\vec{j}_k = \frac{e^{i\omega t}\sigma_k}{r}\left[\gamma(z) + v_k\alpha(z)\right]\hat{\theta} \tag{28}$$

Therefore, the total current passing through the area bounded by the path abcd is

$$\int_{A_{abcd}} \vec{j}\cdot d\vec{A} = e^{i\omega t}\sum_{k=1}^{n}\sigma_k\int_{r_k}^{r_{k+1}}\frac{dr}{r}\int_0^z\left[\gamma(z') + v_k\alpha(z')\right]dz'$$

$$= e^{i\omega t}\sum_{k=1}^{n}\sigma_k \ln\left(\frac{r_{k+1}}{r_k}\right)\int_0^z\left[\gamma(z') + v_k\alpha(z')\right]dz' \tag{29}$$

The left-hand side of equation (26) can be evaluated by making the following substitutions:

$$\vec{H} = \frac{\vec{B}}{\mu}$$

$$\vec{B} = \frac{\alpha(z)}{r}e^{i\omega t}\hat{r}$$

Therefore,

$$\int_{cd} \vec{H} \cdot d\ell = \frac{e^{i\omega t}}{\mu} \alpha(z) \int_{r_1}^{r_{n+1}} \frac{dr}{r}$$

$$= \frac{e^{i\omega t}}{\mu} \ln\left(\frac{r_{n+1}}{r_1}\right) \alpha(z) \tag{30}$$

Similarly,

$$\int_{ab} H \cdot d\ell = -\frac{e^{i\omega t}}{\mu} \ln\left(\frac{r_{n+1}}{r_1}\right) \alpha(0) \tag{31}$$

Inserting equations (29), (30), and (31) into equation (26) results in

$$e^{i\omega t} \ln\left(\frac{r_{n+1}}{r_1}\right)\left[\alpha(z) - \alpha(0)\right] = e^{i\omega t} \sum_{k=1}^{n} \mu\sigma_k \ln\left(\frac{r_{k+1}}{r_k}\right) \int_0^z \left[\gamma(z') + v_k \alpha(z')\right] dz'$$

Differentiating this equation twice with respect to the axial coordinate z and removing the factor $e^{i\omega t}$ result in

$$\ln\left(\frac{r_{n+1}}{r_1}\right) \frac{d^2\alpha}{dz^2} = \sum_{k=1}^{n} \mu\sigma_k \ln\left(\frac{r_{k+1}}{r_k}\right)\left(\frac{d\gamma}{dz} + v_k \frac{d\alpha}{dz}\right)$$

Substituting for $d\gamma/dz$ in equation (24) gives

$$\ln\left(\frac{r_{n+1}}{r_1}\right) \frac{d^2\alpha}{dz^2} = \sum_{k=1}^{n} \mu\sigma_k \ln\left(\frac{r_{k+1}}{r_k}\right)\left(i\omega\alpha + v_k \frac{d\alpha}{dz}\right) \tag{32}$$

It is convenient at this point to define a flow magnetic Reynolds number Re_{mv}, a frequency magnetic Reynolds number $Re_{m\omega}$, and a dimensionless axial coordinate ζ:

$$Re_{mv} = \frac{\mu C}{\ln\left(\frac{r_{n+1}}{r_1}\right)} \sum_{k=1}^{n} \sigma_k v_k \ln\left(\frac{r_{k+1}}{r_k}\right) \tag{33}$$

$$Re_{m\omega} = \frac{\mu C^2 \omega}{\pi \ln\left(\frac{r_{n+1}}{r_1}\right)} \sum_{k=1}^{n} \sigma_k \ln\left(\frac{r_{k+1}}{r_k}\right) \tag{34}$$

$$\zeta = \frac{z}{C} \tag{35}$$

The inclusion of the factor $1/\pi$ in the definition of $Re_{m\omega}$ is explained in the section COMPARISON WITH TRAVELING-FIELD PUMPS and has to do with comparison of single-phase and traveling-field electromagnetic pumps.

With these definitions, equation (32) can be written

$$\frac{d^2\alpha}{d\zeta^2} - Re_{mv} \frac{d\alpha}{d\zeta} - i\pi Re_{m\omega} \alpha = 0 \tag{36}$$

The general solution to equation (36) is

$$\alpha(\zeta) = C_1 e^{Re'_m \zeta} + C_2 e^{Re''_m \zeta} \tag{37}$$

where

$$Re'_m = \frac{1}{2}\left[Re_{mv} + \sqrt{(Re_{mv})^2 + 4i\pi Re_{m\omega}}\right]$$

$$Re''_m = \frac{1}{2}\left[Re_{mv} - \sqrt{(Re_{mv})^2 + 4i\pi Re_{m\omega}}\right]$$

A convenient solution for the magnetic-field strength $\vec{B}$ is therefore possible by defining flow and frequency magnetic Reynolds numbers in the manner prescribed by equations (33) and (34). Remember, however, that these are average quantities and that in obtaining the solution given by equation (37) only the integral form of Ampere's law has

been used. Except in the ideal case where the only medium contained in the annulus is the fluid to be pumped, the differential form of Ampere's law will give a current density that is an average of the current densities of the various media in the annulus. The solution is therefore approximate. For more accurate computation of the current density in any particular material within the annulus, Ohm's law will be used. In this sense, the analysis presented herein is similar to analyses for which magnetic-Reynolds number effects can be neglected. The difference is that the magnetic field $\vec{B}$ is not assumed but is obtained on the basis of the average magnetic Reynolds numbers Re_{mv} and $Re_{m\omega}$.

Boundary Conditions

After the form of the magnetic field as given by equation (37) is determined, appropriate boundary conditions must be assigned at the annulus inlet and outlet in order to determine the constants C_1 and C_2. As a result of doing this for both pumps A and B, the magnetic and electric fields will be completely determined.

Substituting equation (37) into equation (24) and integrating with respect to ζ give

$$\gamma(\zeta) = i\omega C\left(\frac{C_1}{Re'_m} e^{Re'_m \zeta} + \frac{C_2}{Re''_m} e^{Re''_m \zeta}\right) \tag{38}$$

For convenience, the complex constants C_1 and C_2 are defined in terms of two other complex constants K_1 and K_2 and the peak magnetic field strength B_c that exists in the low radius portion of the magnetic core on the inlet side of the annulus (see fig. 4). The magnetic-field strength $\vec{B}_c$ is assumed to be given by

$$\vec{B}_c = B_c e^{i\omega t}\hat{k} \tag{39}$$

The definitions of the constants K_1 and K_2 are as follows:

$$\left.\begin{aligned} C_1 &= K_1 B_c \\ C_2 &= K_2 B_c \end{aligned}\right\} \tag{40}$$

Therefore,

$$\vec{B} = \frac{B_c e^{i\omega t}}{r}\left(K_1 e^{Re'_m \zeta} + K_2 e^{Re''_m \zeta}\right)\hat{r} \tag{41}$$

and

$$\vec{E} = \frac{i\omega C B_c e^{i\omega t}}{r}\left(\frac{K_1}{Re'_m} e^{Re'_m \zeta} + \frac{K_2}{Re''_m} e^{Re''_m \zeta}\right)\hat{\theta} \tag{42}$$

For both pumps A and B, the appropriate boundary condition at the annulus inlet is the same. This boundary condition is derived by taking the line integral of the electric field strength E_i at the annulus inlet around the closed paths 1A or 1B (see fig. 4). Faraday's law (eq. (1)) can then be used to relate the quantities E_i and B_c:

$$\left.\begin{aligned} e^{i\omega t}\int_0^{2\pi} E_i r\, d\theta &= -\int_{A_c} \frac{\partial \vec{B}_c}{dt}\cdot d\vec{A} \\ &= -i\omega e^{i\omega t}\int_{A_c} B_c\, dA \\ 2\pi r E_i &= -i\omega B_c A_c \\ &= -i\omega B_c \pi a^2 \\ E_i &= -\frac{i\omega B_c}{r}\left(\frac{a^2}{2}\right) \end{aligned}\right\} \tag{43}$$

Equating equations (42) and (43) for $\zeta = 0$ yields

$$C\left(\frac{K_1}{Re'_m} + \frac{K_2}{Re''_m}\right) = -\frac{a^2}{2} \tag{44}$$

For pump A, a second boundary condition is obtained by taking the line integral of the magnetic-field intensity around path 2A (see fig. 4(a)). Path 2A consists of the segment l_s in the magnetic core on the outlet side of the annulus and the radial path $r_{n+1} \rightarrow r_1$ through the annulus at $\zeta = 1$. That there is no current flow in the fluid or outlet pipes has already been assumed. Therefore, using Ampere's law (eq. (2)) results in

$$\frac{B_s}{\mu_c} l_s - \int_{r_{n+1}}^{r_1} \frac{B_o \, dr}{\mu} = 0$$

At $\zeta = 1$

$$B = B_o e^{i\omega t} \hat{r} = \frac{B_c}{r} \left(K_{1,A} e^{Re'_m} + K_{2,A} e^{Re''_m} \right) e^{i\omega t} \hat{r}$$

Therefore,

$$K_{1,A} e^{Re'_m} + K_{2,A} e^{Re''_m} = \frac{B_s}{B_c} \left(\frac{\mu l_s}{\mu_c} \right) \frac{1}{\frac{r_1}{r_{n+1}}} \tag{45}$$

For most cases of interest, the quantity μ/μ_c is generally much less than 1, and the right-hand side of equation (45) is approximately zero. Equation (45), therefore, can be approximated by

$$K_{1,A} e^{Re'_m} + K_{2,A} e^{Re''_m} = 0 \tag{46}$$

Solving equations (44) and (46) simultaneously results in the following values of $K_{1,A}$ and $K_{2,A}$:

$$\left.\begin{aligned} K_{1,A} &= \frac{iRe_m \omega \pi a^2}{2C \left(Re''_m - Re'_m e^{Re'_m - Re''_m} \right)} \\ K_{2,A} &= \frac{iRe_m \omega \pi a^2}{2C \left(Re'_m - Re''_m e^{Re''_m - Re'_m} \right)} \end{aligned}\right\} \text{Pump A} \tag{47}$$

The second boundary condition for pump B is obtained by equating the line integral of the electric-field strength around path 2B to the negative rate of change of magnetic flux through the area enclosed by path 2B. Since no flux passes through this area, the appropriate boundary condition at $\zeta = 1$ is that the electric-field intensity be zero. Therefore,

$$\frac{K_{1,B}}{Re'_m} e^{Re'_m} + \frac{K_{2,B}}{Re''_m} e^{Re''_m} = 0 \tag{48}$$

Solving equations (44) and (48) simultaneously results in the following values of $K_{1,B}$ and $K_{2,B}$:

$$\left.\begin{aligned} K_{1,B} &= \frac{iRe_m \omega \pi a^2}{2CRe''_m\left(1 - e^{Re'_m - Re''_m}\right)} \\ K_{2,B} &= \frac{iRe_m \omega \pi a^2}{2CRe'_m\left(1 - e^{Re''_m - Re'_m}\right)} \end{aligned}\right\} \text{Pump B} \tag{49}$$

If the excitation coil of either pumps A or B is assumed to have N turns and carries a peak current $|I|$, the number of excitation ampere-turns is

$$N\vec{I} = NIe^{i\omega t}\hat{\theta} \tag{50}$$

Again the use of Ampere's law to compute the line integral of the magnetic intensity around paths 3A or 3B gives

$$\frac{B_c}{\mu} \ln\left(\frac{r_{n+1}}{r_1}\right)(K_1 + K_2) = NI \tag{51}$$

In deriving equation (51), the line integral of magnetic intensity over that portion of paths 3A or 3B within the magnetic core has again been assumed small as compared with the magnetic intensity integral within the annulus. Also, current flow in the fluid and pipes on the inlet side of the annulus and fringing flux on both sides of the annulus have been neglected. Equation (51) provides a means for relating B_c to the excitation ampere turns NI, or vice versa. Since K_1 and K_2 are complex, $\vec{B}_c$ and $N\vec{I}$ will, in general, have different phases. Equation (51), therefore, also determines either the phase of $\vec{B}_c$ or $N\vec{I}$, given the phase of the other. The choice of B_c as a real number is convenient in order to simplify the equations resulting from the boundary conditions.

Comparison of equations (47) and (49) indicates that both pumps should have identical characteristics in the limiting case where $Re'_m = -Re''_m$. This behavior will occur, for

instance, if $Re_{m\omega}$ is very high in comparison with Re_{mv}. Such circumstances result when the excitation frequency ω is high and/or when the fluid velocity is low.

It is notable that, in pump A, the outlet boundary condition (eq. (46)) requires that the magnetic field strength B_o at the outlet be zero. This boundary condition is not necessarily the case for pump B, except for high values of the ratio $Re_{m\omega}/Re_{mv}$. Both pumps, however, have the same boundary conditions at the annulus inlet (eq. (44)). From the discussion presented in the first section and because the square of the outlet magnetic field strength B_o^2 is a minimum (namely zero), pump A should be more capable of producing force than pump B. Because of these considerations, pump A is expected to have a higher ideal efficiency than pump B, which is, indeed, the case. Pump B, however, offers a simpler outlet duct construction and might be preferable in some instances.

Performance Parameters

Some important parameters in the evaluation of electromagnetic pumps are efficiency, power factor, and peak magnetic-field strength for a given pressure rise and flow rate. In order to determine the efficiency of single-phase pumps, the losses, electrical and viscous, which result from pump operation at the specified conditions must be determined. The electrical losses in the annulus and the peak magnetic-field strength B_c can be calculated from three dimensionless functions φ, χ, and ψ, which will be defined in this section. Dimensionless core magnetic-field strength and power-factor functions will also be developed, from which calculations of the necessary excitation ampere-turns and voltage requirements can be made.

The real, dimensionless, functions $b_R(\zeta)$, $b_I(\zeta)$, $e_R(\zeta)$, and $e_I(\zeta)$ are defined so that

$$b_R(\zeta) + ib_I(\zeta) = -\frac{C}{a^2}\left(K_1 e^{Re'_m \zeta} + K_2 e^{Re''_m \zeta}\right) \tag{52}$$

$$e_R(\zeta) + ie_I(\zeta) = \frac{iC}{a^2}\left(\frac{K_1}{Re'_m} e^{Re'_m \zeta} + \frac{K_2}{Re''_m} e^{Re''_m \zeta}\right) \tag{53}$$

Comparison of equations (52) and (53) with equations (41), (43), (47), and (49) shows that the functions $b_R(\zeta)$, $b_I(\zeta)$, $e_R(\zeta)$, and $e_I(\zeta)$ depend only on ζ and the two magnetic Reynolds numbers $Re_{m\omega}$ and Re_{mv}. Magnetic and electric field strengths $\vec{B}$ and $\vec{E}$ (eqs. (41) and (42)) can be written

$$\mathcal{R}\vec{B} = -\mathcal{R}\left\{\left(\frac{a^2 B_c}{C}\right)\frac{e^{i\omega t}}{r}\left[b_R(\zeta) + ib_I(\zeta)\right]\right\}\hat{r}$$

$$= -\left(\frac{a^2 B_c}{C}\right)\frac{1}{r}\left[b_R(\zeta)\cos\,\omega t - b_I(\zeta)\sin\,\omega t\right]\hat{r} \tag{54}$$

$$\mathcal{R}\vec{E} = \mathcal{R}\left\{\frac{\left(a^2\omega B_c\right)e^{i\omega t}}{r}\left[e_R(\zeta) + ie_I(\zeta)\right]\right\}\hat{\theta}$$

$$= \frac{\left(a^2\omega B_c\right)}{r}\left[e_R(\zeta)\cos\,\omega t - e_I(\zeta)\sin\,\omega t\right]\hat{\theta} \tag{55}$$

In equations (54) and (55) the quantity B_c has been taken to be a real number, and without loss of generality only the real part of $\vec{B}_c$ is considered to actually exist. It is therefore appropriate to take only the real parts of $\vec{B}$ and $\vec{E}$ as defined in equations (41) and (42). The current density $\vec{j}_k$ in the k^{th} medium within the annulus is

$$\vec{j}_k = \sigma_k\left(\vec{E} + \vec{v}_k \times \vec{B}\right)$$

$$= \frac{\hat{\theta}}{r}\left(\sigma_k a^2 B_c\right)\left\{\cos\,\omega t\left[\omega e_R(\zeta) - \frac{v_k}{C}b_R(\zeta)\right] - \sin\,\omega t\left[\omega e_I(\zeta) - \frac{v_k}{C}b_I(\zeta)\right]\right\} \tag{56}$$

The amount of work done per unit time on medium k by the electromagnetic field is obtained by integrating the product of the Lorentz force per unit volume $\vec{j}_k \times \vec{B}$ and the velocity v_k over the k^{th} volume and averaging the result over a period of time $2\pi/\omega$; that is, work done per unit time on medium k is

$$W_{m,k} = \frac{\omega}{2\pi}\int_0^{2\pi/\omega}\int_0^{C}\int_0^{2\pi}\int_{r_k}^{r_{k+1}}\left(\vec{j}_k \times \vec{B}\right)\cdot\vec{v}_k r\,dr\,d\theta\,dz\,dt$$

$$= \pi\sigma_k\left(a^2 B_c\right)^2 \ln\left(\frac{r_{k+1}}{r_k}\right)\left(\omega v_k \chi - \frac{v_k^2}{C}\psi\right) \tag{57}$$

Similarly, the electrical losses L_k in medium k are computed by integrating the power losses $\left(j_k \cdot j_k\right)/\sigma_k$ per unit volume over the k^{th} volume and taking the time average

$$L_{m,k} = \frac{\omega}{2\pi} \int_0^{2\pi/\omega} \int_0^{C} \int_0^{2\pi} \int_{r_k}^{r_{k+1}} \frac{\left(\vec{j}_k \cdot \vec{j}_k\right)}{\sigma_k} r \, dr \, d\theta \, dz \, dt$$

$$= \pi\sigma_k \left(a^2 B_c\right)^2 \ln\left(\frac{r_{k+1}}{r_k}\right) \left(\omega^2 C\varphi - 2\omega v_k \chi + \frac{v_k^2}{C}\psi\right) \tag{58}$$

The quantities φ, χ, and ψ are dimensionless functions of the two magnetic Reynolds numbers $Re_{m\omega}$ and Re_{mv} and are defined as

$$\varphi = \int_0^1 \left[e_R^2(\zeta) + e_I^2(\zeta)\right] d\zeta \tag{59}$$

$$\chi = \int_0^1 \left[e_R(\zeta) b_R(\zeta) + e_I(\zeta) b_I(\zeta)\right] d\zeta \tag{60}$$

$$\psi = \int_0^1 \left[b_R^2(\zeta) + b_I^2(\zeta)\right] d\zeta \tag{61}$$

The total work W_m done per unit time on all the media in the annulus is then

$$W_m = \sum_{k=1}^{n} W_{m,k} = \pi\left(a^2 B_c\right)^2 \left[\chi \sum_{k=1}^{n} (\sigma_k v_k \omega) \ln\left(\frac{r_{k+1}}{r_k}\right) - \psi \sum_{k=1}^{n} \left(\frac{\sigma_k v_k^2}{C}\right) \ln\left(\frac{r_{k+1}}{r_k}\right)\right] \tag{62}$$

and, similarly, the total electrical loss L_m in the annulus is

$$L_m = \sum_{k=1}^{n} L_{m,k}$$

$$= \pi\left(a^2 B_c\right)^2 \left[\varphi \sum_{k=1}^{n} \left(\sigma_k \omega^2 C\right) \ln\left(\frac{r_{k+1}}{r_k}\right) - 2\chi \sum_{k=1}^{n} \left(\sigma_k v_k \omega\right) \ln\left(\frac{r_{k+1}}{r_k}\right) \right.$$

$$\left. + \psi \sum_{k=1}^{n} \left(\frac{\sigma_k v_k^2}{C}\right) \ln\left(\frac{r_{k+1}}{r_k}\right) \right] \qquad (63)$$

The developed pressure in the k^{th} medium can be obtained from

$$\Delta p_{m,k} = \frac{W_{m,k}}{\pi\left(r_{k+1}^2 - r_k^2\right) v_k} \qquad (64)$$

For most pump designs, the peak flux density in the magnetic core will occur in the low radius portion. The magnitude of B_c is, therefore, important in order to determine how close to saturation the pump is. A convenient nondimensionalization of B_c is provided by taking the line integral of the magnetic intensity around path 3A or 3B (see fig. 4) and equating this to the excitation ampere turns $N\vec{I}$. Equation (50) can be written

$$N\vec{I} = \left(NI_R \cos \omega t - NI_I \sin \omega t\right)\hat{\theta} \qquad (65)$$

Again, only the real part of $N\vec{I}$ is used. Computing the line integral

$$\oint_{\text{path 3A, B}} \frac{\vec{B}}{\mu} \cdot d\vec{\ell}$$

and equating the result to equation (65), using equation (54), result in

$$NI_R = -B_c \left[\frac{a^2 \ln\left(\frac{r_{n+1}}{r_1}\right)}{\mu C} \right] b_R(0) \tag{66}$$

$$NI_I = -B_c \left[\frac{a^2 \ln\left(\frac{r_{n+1}}{r_1}\right)}{\mu C} \right] b_I(0) \tag{67}$$

$$NI = \sqrt{(NI_R)^2 + (NI_I)^2}$$

$$= B_c \left[\frac{a^2 \ln\left(\frac{r_{n+1}}{r_1}\right)}{\mu C} \right] \sqrt{b_R^2(0) + b_I^2(0)}$$

$$\frac{B_c}{NI} \left[\frac{a^2 \ln\left(\frac{r_{n+1}}{r_1}\right)}{\mu C} \right] = \frac{1}{\sqrt{b_R^2(0) + b_I^2(0)}} \equiv \beta \tag{68}$$

Equation (68) defines β, a nondimensional peak magnetic-field strength, in terms of the peak values of the low-radius core magnetic-field strength and the excitation ampere-turns. The quantities $b_R(0)$ and $b_I(0)$, and therefore β, are functions of the two magnetic Reynolds numbers $Re_{m\omega}$ and Re_{mv} only.

The voltage V necessary to produce a peak current I in an exciting coil of N turns can be computed from Ohm's law (eq. (5)). The electric field $\vec{E}$ in this case is the sum of the applied potential field produced by V and the electric field $\vec{E}_i$ resulting from the presence of a time-varying magnetic field $\vec{B}_c$. Since the velocity of the coils is zero, Ohm's law reduces to

$$\vec{j}_e = \sigma_e\left(\vec{E}_i + \nabla\varphi_v\right) \tag{69}$$

The quantities $\vec{j}_e$, $\vec{E}_i$, and $\nabla\varphi_V$ have components in the θ direction only and are proportional to $e^{i\omega t}$. Therefore,

$$\vec{j}_e = j_e e^{i\omega t}\hat{\theta} \tag{70}$$

$$\vec{E}_i = E_i e^{i\omega t}\hat{\theta} \tag{71}$$

$$\nabla\varphi_V = \frac{V_t}{2\pi r} e^{i\omega t}\hat{\theta} \tag{72}$$

For the usual case in which the exciting coil is made of many turns N, the current density j_e is approximately constant. Furthermore, since $\vec{j}_e$ and $N\vec{I}$ are in phase, $j_e = NI/hw$, where h is the coil height and w is the coil width (see fig. 2). Using equations (65), (66), and (67) and separating j_e into real and imaginary parts result in

$$j_{e,R} = -\frac{B_c}{hw}\left[\frac{a^2 \ln\left(\frac{r_{n+1}}{r_1}\right)}{\mu C}\right] b_R(0) \tag{73}$$

$$j_{e,I} = -\left[\frac{B_c}{hw}\,\frac{a^2 \ln\left(\frac{r_{n+1}}{r_1}\right)}{\mu C}\right] b_I(0) \tag{74}$$

where

$$j_e = j_{e,R} + ij_{e,I} \tag{75}$$

The induced electric field $\vec{E}_i$ is computed using Faraday's law (eq. (1)).

$$E_i = -\frac{i\omega a^2}{2r} B_c \tag{76}$$

Inserting equations (73) and (74) into equation (75), equation (75) into equation (70), equation (76) into equation (71), and combining the resulting quantities as in equation (69) give

$$-\frac{B_c}{hw}\left[\frac{a^2 \ln\left(\frac{r_{n+1}}{r_1}\right)}{\mu C}\right]\left[b_R(0)\cos\omega t - b_I(0)\sin\omega t\right] = \sigma_e\left(\frac{V_t}{2\pi r} + \frac{\omega a^2}{2r} B_c \sin\omega t\right)$$

so that

$$V_t = B_c \cos\omega t\left\{-\frac{2r}{\sigma_e}\left[\frac{\pi a^2 \ln\left(\frac{r_{n+1}}{r_1}\right)}{\mu Chw}\right] b_R(0)\right\} + B_c \sin\omega t\left\{+\frac{2r}{\sigma_e}\left[\frac{\pi a^2 \ln\left(\frac{r_{n+1}}{r_1}\right)}{\mu Chw}\right] b_I(0) - \pi a^2\omega\right\}$$

(77)

Defining a power factor function PFF such that

$$PFF = \frac{-b_R(0)}{\sqrt{b_R^2(0) + b^2(0)}} = -\beta b_R(0) \tag{78}$$

equation (77) becomes

$$V_t = B_c \cos\omega t\left\{\frac{2r}{\sigma_e}\left[\frac{\pi a^2 \ln\left(\frac{r_{n+1}}{r_1}\right)}{\mu Chw}\right]\left(\frac{PFF}{\beta}\right)\right\}$$

$$- B_c \sin\omega t\left\{\frac{2r}{\sigma_e}\left[\frac{\pi a^2 \ln\left(\frac{r_{n+1}}{r_1}\right)}{\mu Chw}\right]\left[\frac{\sqrt{1 - (PFF)^2}}{\beta}\right] + \pi a^2\omega\right\} \tag{79}$$

The quantity V_t defined in equation (77) is obviously the number of applied volts per turn of the coil. If turn j of the coil has a mean radius $r_{e,j}$ and if all N turns are connected in series, then the voltage V that must be applied to the coils is

$$V = B_c \cos \omega t \left\{ \frac{2}{\sigma_e} \left[\frac{\pi a^2 \ln\left(\frac{r_{n+1}}{r_1}\right)}{\mu Chw} \right] \frac{PFF}{\beta} \sum_{j=1}^{N} r_{e,j} \right\}$$

$$- B_c \sin \omega t \left\{ \frac{2}{\sigma_e} \left[\frac{\pi a^2 \ln\left(\frac{r_{n+1}}{r_1}\right)}{\mu Chw} \right] \left[\frac{\sqrt{1 - (PFF)^2}}{\beta} \right] \sum_{j=1}^{N} r_{e,j} + N\pi a^2 \omega \right\} \qquad (80)$$

The root-mean-square value of the voltage is

$$V_{rms} = 0.707\, B_c \sqrt{\left\{ \frac{2}{\sigma_e} \left[\frac{\pi a^2 \ln\left(\frac{r_{n+1}}{r_1}\right)}{\mu Chw} \right] \left(\frac{PFF}{\beta}\right) \sum_{j=1}^{N} r_{e,j} \right\}^2 + \left\{ \frac{2}{\sigma_e} \left[\frac{\pi a^2 \ln\left(\frac{r_{n+1}}{r_1}\right)}{\mu Chw} \right] \left[\frac{\sqrt{1 - (PFF)^2}}{\beta} \right] \sum_{j=1}^{N} r_{e,j} + N\pi a^2 \omega \right\}^2} \qquad (81)$$

Besides the electrical losses in the fluid and duct walls, additional losses incurred in electromagnetic pumps are the coil electrical losses and the viscous losses resulting from the flow of the pumped fluid in the thin annulus. For constant coil current density j_e the coil electrical losses are

$$L_e \cong \frac{\pi \left(r_{e,o}^2 - r_{e,i}^2\right) w j_e^2}{2\sigma_e} \qquad (82)$$

where $r_{e,i}$ is the minimum coil radius and $r_{e,o}$ is the maximum coil radius. Substituting equations (73) and (74) into equation (82) yields

$$L_e = \frac{1}{2\sigma_e}\left[\frac{B_c a^2 \ln\left(\frac{r_{n+1}}{r_1}\right)}{hw\mu C\beta}\right]^2 \pi\left(r_{e,o}^2 - r_{e,i}^2\right)w \tag{83}$$

If fluid flow in the annulus is turbulent, which is normally the case, and if the magnetic field in the annulus is not too strong, effects of the magnetic field on the viscous losses can be neglected. In this case, ordinary turbulent flow formula (ref. 3) can be used. If the Reynolds number Re_k for the k^{th} fluid in the annulus is defined as

$$Re_k = \frac{2\rho_k v_k (r_{k+1} - r_k)}{\mu_{f,k}} \tag{84}$$

a friction coefficient $C_{f,k}$ can be found from the following

$$C_{f,k} = \frac{0.3164}{Re_k^{0.25}} \qquad \text{for} \quad 2(10^3) < Re_k < 10^5 \tag{85}$$

$$C_{f,k} = 0.0032 + \frac{0.221}{Re_k^{0.237}} \qquad \text{for} \quad Re_k > 10^5 \tag{86}$$

The viscous losses in the k^{th} medium are

$$L_{H,k} = \left(\frac{C_{f,k}\rho_k v_k^2}{8}\right)\left[2\pi C(r_{k+1} + r_k)\right]v_k \tag{87}$$

The total viscous losses are, therefore,

$$L_H = \sum_{k=1}^{n} L_{H,k} = 2\pi C \sum_{k=1}^{n}\left(\frac{C_{f,k}\rho_k v_k^2}{8}\right)(r_{k+1} + r_k)v_k \tag{88}$$

The pressure drop in the k^{th} medium is

$$\Delta p_{H,k} = \frac{W_{H,k}}{\pi\left(r_{k+1}^2 - r_k^2\right)v_k} \tag{89}$$

It is understood that, if the k^{th} medium is not a fluid, equations (87) and (89) have no meaning.

The efficiency of a particular pumping configuration is defined as the net amount of work done per unit time by the pump W divided by the input power $\mathscr{P}$ to the pump. The net amount of work done per unit time is the difference between the amount of work done by the electromagnetic field W_m and the viscous losses W_H:

$$W = W_m - W_H \tag{90}$$

Since the input power to the pump is electrical in nature, $\mathscr{P}$ is the sum of the work done per unit time by the magnetic field W_m plus all the electrical losses incurred:

$$\mathscr{P} = W_m + L_m + L_e \tag{91}$$

The efficiency is, therefore

$$\eta = \frac{W}{\mathscr{P}}(100) \equiv \frac{W_m - W_H}{W_m + L_m + L_e}(100) \tag{92}$$

The aim of this section has been to develop equations that can be used to obtain the performance of single-phase pumps. Those parameters that are peculiar to the single-phase pumping concept have been given in dimensionless form. These dimensionless quantities, along with the physical and geometrical properties of the system, can be used to compute the real parameters that they represent. Other parameters of interest that do not depend on the electromagnetic field have been presented in dimensional form.

PERFORMANCE CHARACTERISTICS AND TRENDS

As was shown previously in the ANALYSIS section, the performance of single-phase pumps depends largely on the two quantities $Re_{m\omega}$ and Re_{mv}. The question that remains is what is the criterion for the selection of these quantities so that a reasonably well-designed pump will result. One criterion would be whether or not pumping could be attained at the selected values of $Re_{m\omega}$ and Re_{mv}. Another might be a crude estimate of efficiency at various values of $Re_{m\omega}$ and Re_{mv}, such as the ideal efficiency.

This section points out performance characteristics and trends for practical ranges of $Re_{m\omega}$ and Re_{mv}. Nondimensionalized curves of ideal output pressure (work), ideal efficiency, and peak core flux density are presented to provide crude estimates of performance. Finally, with these curves as a guide, nonideal performance effects are calculated for a sample pump.

Ideal Quantities

In obtaining a good pump design, obtaining the best efficiency compatible with a given developed pressure and flow rate is of primary interest. This section develops expressions for dimensionless developed pressure (work) and ideal efficiency so that best performance points can be estimated with relative ease.

Ideal developed pressure, or power. - The ideal developed pressure Δp_{id} of an electromagnetic pump is defined as that pressure difference between pump inlet and outlet that would arise if viscous losses were zero and if the fluid were the only medium present in the annulus. Ideal efficiency will be defined in a similar manner such that the viscous loss term W_H and the coil electrical loss term L_e in equation (92) are both zero. Furthermore, the work done by the electromagnetic field W_m and the electrical losses associated with the presence of the electromagnetic field will be calculated on the basis of a single conducting medium in the annulus, namely, the pumped fluid. For this special case the magnetic Reynolds numbers $Re_{m\omega}$ and Re_{mv} (eqs. (33) and (34)) reduce to

$$Re^*_{m\omega} = \frac{\mu\sigma_f C^2 \omega}{\pi} \tag{93}$$

$$Re^*_{mv} = \mu\sigma_f v_f C \tag{94}$$

The subscript f is used herein, rather than an index k since only one medium is present. In this special case the current density $\vec{j}_f$ can be computed from Ampere's law as well as Ohm's law. From Ampere's law the following is obtained:

$$\vec{j}_f = \frac{1}{\mu}\frac{\partial B}{\partial z}\hat{\theta}$$

since $\vec{B} = B\hat{r}$. The pressure developed in the length C is then

$$\Delta p_{id}(t) = \frac{-1}{\mu\pi\left(r_{f,o}^2 - r_{f,i}^2\right)} \int_{r_{f,i}}^{r_{f,o}} \int_0^{2\pi} \int_0^C B \frac{\partial B}{\partial z} \, r \, dz \, d\theta \, dr$$

$$= \frac{-1}{2\mu\pi\left(r_{f,o}^2 - r_{f,i}^2\right)} \int_{r_{f,i}}^{r_{f,o}} \int_0^{2\pi} \int_0^C \frac{\partial (B^2)}{\partial z} \, r \, dz \, d\theta \, dr$$

$$= \frac{1}{\mu\left(r_{f,o}^2 - r_{f,i}^2\right)} \int_{r_{f,i}}^{r_{f,o}} \left[B^2(0) - B^2(C)\right] r \, dr \qquad (95)$$

Substituting equation (54) into equation (95) gives

$$\Delta p_{id}(t) = \left(\frac{a^2 B_c}{C}\right)^2 \frac{1}{\mu\left(r_{f,o}^2 - r_{f,i}^2\right)} \int_{r_{f,i}}^{r_{f,o}} \frac{dr}{r} \left\{\cos^2\omega t\left[b_R^2(0) - b_R^2(C)\right]\right.$$

$$\left. + \sin^2\omega t\left[b_I^2(0) - b_I^2(C)\right] - 2 \sin \omega t \cos \omega t\left[b_R(0)b_I(0) - b_R(C)b_I(C)\right]\right\}$$

Averaging $\Delta p_{id}(t)$ over a time period $2\pi/\omega$ yields

$$\Delta p_{id} \equiv \frac{\omega}{2\pi} \int_0^{2\pi/\omega} \Delta p_{id}(t) dt$$

$$= \frac{\left(\frac{a^2 B_c}{C}\right)^2}{2\mu\left(r_{f,o}^2 - r_{f,i}^2\right)} \ln\left(\frac{r_{f,o}}{r_{f,i}}\right) \left\{\left[b_R^2(0) + b_I^2(0)\right] - \left[b_R^2(C) + b_I^2(C)\right]\right\} \qquad (96)$$

Equation (96) gives Δp_{id} as a difference in magnetic pressures between inlet and outlet. From equation (68),

$$\frac{a^2 B_c}{C} = \frac{\mu(NI)\beta}{\ln\left(\frac{r_{f,o}}{r_{f,i}}\right)}$$

Therefore,

$$\Delta p_{id} = \frac{\mu(NI)^2\beta^2\left\{\left[b_R^2(0) + b_I^2(0)\right] - \left[b_R^2(C) + b_I^2(C)\right]\right\}}{2\left(r_{f,o}^2 - r_{f,i}^2\right)\ln\left(\frac{r_{f,o}}{V_{f,i}}\right)} \tag{97}$$

If a dimensionless output pressure $\Delta\bar{p}_{id}$ is defined so that

$$\Delta\bar{p}_{id} = \frac{2\,\Delta p_{id}\left(r_{f,o}^2 - r_{f,i}^2\right)\ln\left(\frac{r_{f,o}}{r_{f,i}}\right)}{\mu(NI)^2} \tag{98}$$

then by using equation (97), the following equation results:

$$\Delta\bar{p}_{id} = \beta^2\left\{\left[b_R^2(0) + b_I^2(0)\right] - \left[b_R^2(C) + b_I^2(C)\right]\right\} \tag{99}$$

The work done per unit time on the fluid by the electromagnetic field is

$$W_{id} = \pi\left(r_{f,o}^2 - r_{f,i}^2\right)\Delta p_{id}(v_f) \tag{100}$$

Defining a dimensionless power $\overline{W}_{id}$ so that

$$\overline{W}_{id} = \frac{2W_{id}\ln\left(\frac{r_{f,o}}{r_{f,i}}\right)}{\mu\pi(NI)^2 v_f} \tag{101}$$

clearly shows that

$$\overline{W}_{id} = \Delta\bar{p}_{id} \tag{102}$$

Therefore, $\Delta\bar{p}_{id}$ can be thought of as either a dimensionless pressure rise or a dimensionless output power. Figure 5 shows dimensionless ideal pressure $\Delta\bar{p}_{id}$ against frequency magnetic Reynolds number $Re^*_{m\omega}$ for several values of the flow magnetic Reynolds number Re^*_{mv}. Figure 5(a) is somewhat more convenient for design calculations; whereas figure 5(b) can be thought of as a dimensionless-head - dimensionless-flow curve. Figure 5(b) is therefore useful in describing the approximate behavior of single-phase pumps in familiar terms. Note that $\Delta\bar{p}_{id}$ is constant over the full range of $Re^*_{m\omega}$ for pump A. This behavior occurs because the quantity $b_R^2(C) + b_I^2(C)$ is zero by virtue of the boundary condition at the annulus outlet as expressed by equation (46). Using this fact and substituting equation (68) into equation (99) give

$$\Delta p_{id} = \beta^2\left(\frac{1}{\beta^2}\right) = 1$$

On the other hand, pump B exhibits a characteristic similar to that of a traveling-field electromagnetic pump. For this pump, a value of the frequency magnetic Reynolds number $\left(Re^*_{m\omega}\right)_{min}$ dependent on the flow magnetic Reynolds number Re^*_{mv} exists, below which pumping is not possible in the ideal case. A plot of $\left(Re^*_{m\omega}\right)_{min}$ as a function of Re^*_{mv} is given in figure 6.

Ideal efficiency. - Figure 7 shows ideal efficiency η_{id} against frequency magnetic Reynolds number $Re^*_{m\omega}$ for several values of the flow magnetic Reynolds number Re^*_{mv}. Both figures 7(a) and (b) are given for the same reasons as given previously with regard to figures 5(a) and (b). Several trends inherent in these curves are worth noting.

First, both pumps A and B perform equally well for high values of the frequency magnetic Reynolds number $Re^*_{m\omega}$ (see fig. 7). This behavior results from the fact that the magnitudes of the complex magnetic Reynolds numbers Re'_m and Re''_m approach each other when $Re_{m\omega}$ becomes much larger than Re_{mv}.

Secondly, single-phase pumps apparently must be operated at flow magnetic Reynolds numbers greater than 1 in order to obtain reasonable efficiencies. For $Re^*_{mv} \leq 1$, values for ideal efficiency η_{id} are less than 32 percent. Real efficiencies can be expected to be even less.

Thirdly, as $Re^*_{m\omega}$ is decreased, the ideal efficiency of pump B decreases and becomes zero at $Re^*_{m\omega} = \left(Re^*_{m\omega}\right)_{min}$. On the other hand, the ideal efficiency of pump A approaches an asymptote as $Re^*_{m\omega}$ is decreased. Also, for sufficiently high values of Re^*_{mv} this asymptote appears to approach its own asymptote of $\left(\eta_{id}\right)_{max} = 50$ percent. To determine whether these conclusions are correct, the ideal output power W_{id} and ideal electrical losses L_{id} in the fluid must be computed, and the values each of these approach as $Re^*_{m\omega}$ approaches zero must be determined.

From equation (41),

$$\vec{B} = \mathcal{R} \frac{B_c e^{i\omega t}}{r} \left[K_1^* e^{(Re_m')^* \zeta} + K_2^* e^{(Re_m'')^* \zeta} \right] \hat{r} \tag{103}$$

The asterisk implies that K_1, K_2, Re_m', and Re_m'' are based on the magnetic Reynolds numbers $Re^*_{m\omega}$ and Re^*_{mv}. In this ideal case the current density $\vec{j}_f$ can be computed from

$$\vec{j}_f = \mathcal{R} \frac{1}{\mu} \frac{\partial B}{\partial z} \hat{\theta}$$

$$= \mathcal{R} \frac{B_c e^{i\omega t}}{\mu C r} \left[K_1^* (Re_m')^* e^{(Re_m')^* \zeta} + K_2^* (Re_m'')^* e^{(Re_m'')^* \zeta} \right] \hat{\theta} \tag{104}$$

The first case to be considered will be where both $Re^*_{m\omega}$ and Re^*_{mv} are small but where the former is much smaller than the latter. An ordering process will be used such that

$$\left.\begin{aligned} Re^*_{mv} &= \mathcal{O}(\epsilon) \\ Re^*_{m\omega} &= \mathcal{O}(\epsilon^3) \\ \frac{Re^*_{m\omega}}{Re^*_{mv}} &= \mathcal{O}(\epsilon^2) \end{aligned}\right\} \tag{105}$$

where $\epsilon \ll 1$. For small but finite Re^*_{mv}, equations (105) should give results that are valid for $Re^*_{m\omega} = 0$. The constants K_1^* and K_2^* can be computed from equations (47). In order to do this, however, estimates of the quantities $(Re_m')^*$ and $(Re_m'')^*$ that are consistent with equations (105) must be obtained first. These can be obtained from the definitions of $(Re_m')^*$ and $(Re_m'')^*$, namely,

$$\left.\begin{aligned}(Re'_m)^* &= \frac{Re^*_{mv}}{2}\left[1 + \sqrt{1 + 4i\pi\left(\frac{Re^*_{m\omega}}{Re^{*2}_{mv}}\right)}\right] \\ (Re''_m)^* &= \frac{Re^*_{mv}}{2}\left[1 - \sqrt{1 + 4i\pi\left(\frac{Re^*_{m\omega}}{Re^{*2}_{mv}}\right)}\right]\end{aligned}\right\} \tag{106}$$

For $\epsilon \ll 1$ the quantity $\sqrt{1 + \mathcal{O}(\epsilon)}$ can be approximated by

$$\sqrt{1 + \mathcal{O}(\epsilon)} \cong 1 + \frac{\mathcal{O}(\epsilon)}{2}$$

Therefore, allowing only terms of order ϵ yields

$$\left.\begin{aligned}(Re'_m)^* &\cong Re^*_{mv} \\ (Re''_m)^* &\cong 0 \\ (Re'_m)^* - (Re''_m)^* &\cong Re^*_{mv}\end{aligned}\right\} \tag{107}$$

For $\epsilon \ll 1$, $e^{\mathcal{O}(\epsilon)}$ is approximately

$$e^{\mathcal{O}(\epsilon)} \cong 1 + \mathcal{O}(\epsilon)$$

Therefore,

$$\left.\begin{aligned}e^{\left[(Re'_m)^* - (Re''_m)^*\right]} &\cong 1 + Re^*_{mv} \\ e^{\left[(Re''_m)^* - (Re'_m)^*\right]} &\cong 1 - Re^*_{mv}\end{aligned}\right\} \tag{108}$$

With equations (107) and (108) the denominators of equations (47) can be computed:

$$\left.\begin{aligned}(Re''_m)^* - (Re'_m)^* e^{\left[(Re'_m)^* - (Re''_m)^*\right]} &\cong 0 - Re^*_{mv}(1 + Re^*_{mv}) \\ (Re'_m)^* - (Re''_m)^* e^{\left[(Re''_m)^* - (Re'_m)^*\right]} &\cong Re^*_{mv}\end{aligned}\right\} \tag{109}$$

Substituting equations (109) into equations (47) results in

$$\left.\begin{aligned}K_1^* &\cong \frac{iRe^*_{m\omega}\pi a^2}{2CRe^*_{mv}(1 + Re^*_{mv})} \\ K_2^* &\cong \frac{iRe^*_{m\omega}\pi a^2}{2CRe^*_{mv}}\end{aligned}\right\} \tag{110}$$

Using equations (107) and (110) in equations (113) and (114) results in

$$\vec{B} \cong \mathscr{R} \frac{B_c \pi a^2 Re^*_{m\omega} \sin \omega t}{2Cr(1 + Re^*_{mv})} (\zeta - 1)\hat{r} \tag{111}$$

$$\vec{j}_f \cong \mathscr{R} \frac{B_c \pi a^2 Re^*_{m\omega} \sin \omega t}{2Cr(1 + Re^*_{mv})} \left(\frac{1}{\mu C}\right)\hat{\theta} \tag{112}$$

If

$$Q = \frac{\pi}{C}\left[\frac{B_c \pi a^2 Re^*_{m\omega}}{2(1 + Re^*_{mv})}\right]^2 \ln\left(\frac{r_{f,o}}{r_{f,i}}\right)$$

then the ideal work W_{id} is given by

$$W_{id} \cong \frac{\omega}{2\pi} \int_0^{2\pi/\omega} \int_V \left(\vec{j}_f \times \vec{B}\right) \cdot \vec{v}_f \, d\tau \, dt$$

$$= Q\left(\frac{v_f}{\mu C}\right) \int_0^1 (1 - \zeta) d\zeta$$

$$\cong Q\left(\frac{v_f}{2\mu C}\right)$$

$$= Q \frac{Re^*_{mv}}{2} \left(\frac{1}{\sigma_f \mu^2 C^2}\right) \tag{113}$$

and the ideal losses are

$$L_{id} \cong \frac{\omega}{2\pi} \int_0^{2\pi/\omega} \int_V \left(\frac{\vec{j} \cdot \vec{j}}{\sigma_f}\right) d\tau \, dt$$

$$= Q\left(\frac{1}{\sigma_f \mu^2 C^2}\right) \int_0^1 d\zeta$$

$$\cong Q \frac{1}{\sigma_f \mu^2 C^2} \tag{114}$$

The ideal efficiency η_{id} is therefore

$$\eta_{id} \cong \frac{W_{id}(100)}{W_{id} + L_{id}}$$

$$= \frac{(Re^*_{mv}/2)(100)}{1 + (Re^*_{mv}/2)}$$

For very small Re^*_{mv} this becomes

$$\eta_{id} \cong \frac{Re^*_{mv}(100)}{2} \tag{115}$$

Therefore, for very small flow and frequency magnetic Reynolds numbers, the ideal efficiency of pump A approaches a value equal to half the flow magnetic Reynolds number Re^*_{mv}. This behavior is reflected in figure 7 for the cases where Re^*_{mv} has the values 0.01 and 0.1.

To determine the behavior at higher values of Re^*_{mv}, the case where $Re^*_{m\omega}$ is much smaller than Re^*_{mv} may again be considered. In this case, equations (107) are still valid. The approximation $e^{Re^*_{mv}} = 1 + Re^*_{mv}$ is no longer appropriate, however. Assume, therefore, that Re^*_{mv} is much larger than 1. The constants K_1^* and K_2^* become

$$\left.\begin{aligned} K_1^* &\cong -\frac{iRe^*_{m\omega}\pi a^2 e^{-Re^*_{mv}}}{2CRe^*_{mv}} \\ K_2^* &\cong \frac{iRe^*_{m\omega}\pi a^2}{2CRe^*_{mv}} \end{aligned}\right\} \tag{116}$$

Equations (103) and (104) then become, approximately

$$\vec{B} = \mathscr{R}\left\{\frac{B_c \pi a^2 Re_{m\omega} \sin \omega t}{2CrRe^*_{mv}}\left[e^{Re_{mv}(\zeta-1)} - 1\right]\hat{r}\right\} \tag{117}$$

$$\vec{j}_f = \mathscr{R}\left\{\frac{B_c \pi a^2 Re^*_{m\omega} \sin \omega t}{2CrRe^*_{mv}}\left[\frac{Re^*_{mv} e^{Re^*_{mv}(\zeta-1)}}{\mu C}\right]\hat{\theta}\right\} \tag{118}$$

If

$$Q' = \frac{\pi}{C}\left(\frac{B_c \pi a^2 Re^*_{m\omega}}{2Re^*_{mv}}\right)^2 \ln\left(\frac{r_{f,o}}{r_{r,i}}\right)$$

then, the ideal work W_{id} is given by

$$W_{id} \cong \frac{\omega}{2\pi} \int_0^{2\pi/\omega} \int_V \left(\vec{j}_f \times \vec{B}\right) \cdot \vec{v}_f \, d\tau \, dt$$

$$= -Q' \left(\frac{v_f}{\mu C}\right) \int_0^1 Re^*_{mv} \left[e^{2Re^*_{mv}(\zeta-1)} - e^{Re^*_{mv}(\zeta-1)} \right] d\zeta$$

$$\cong \frac{Q'}{2} \left(\frac{v_f}{\mu C}\right) \tag{119}$$

The terms containing $e^{-2Re^*_{mv}}$ and $e^{-Re^*_{mv}}$ have been neglected in computing equation (119) since $Re^*_{mv} >> 1$. The ideal losses L_{id} are obtained from

$$L_{id} \cong \frac{\omega}{2\pi} \int_0^{2\pi/\omega} \int_V \left(\frac{\vec{j}_f \cdot \vec{j}_f}{\sigma_f}\right) d\tau \, dt$$

$$= Q' \left(\frac{1}{\sigma_f \mu^2 C^2}\right) \int_0^1 \left(Re^*_{mv}\right)^2 e^{2Re^*_{mv}(\zeta-1)} \, d\zeta$$

$$\cong Q' \left(\frac{1}{\sigma_f \mu^2 C^2}\right) \left[\frac{(Re^*_{mv})}{2}\right]$$

$$= \frac{Q'}{2} \left(\frac{v_f}{\mu C}\right) \tag{120}$$

In the limiting case of $Re^*_{mv} >> 1$ and $Re^*_{m\omega} << 1$, the work done on the fluid and the electrical losses in the fluid become of equal magnitude for pump A. Figure 7 shows that, in this limit, the highest efficiencies are obtained. It can therefore be concluded that the maximum efficiency obtainable is 50 percent. By inference, this might seem a severe limitation in light of the fact that the maximum obtainable efficiency for traveling-field induction pumps is 100 percent. This conclusion is valid if the fluid electrical losses are much larger than other losses. If coil electrical losses are significant, however, which is quite often the case, highest efficiencies are usually obtained in those

pumps for which these losses are held at a minimum. The last section shows that the coil losses in single-phase induction pumps can be made considerably smaller than is possible in traveling-field pumps. This is possible primarily because coil temperatures and current densities can be made smaller.

Magnetic Flux Density Considerations

The value of the magnetic flux density B_c in the low-radius portion of the core is important for two reasons. First, if B_c is too large, the magnetic core is likely to saturate. Secondly, if B_c is large in comparison with the magnetic-field strength $\vec{B}$ in the annulus, the magnetic intensity drop over those portions of paths 2A, 3A, and 3B that passes through the magnetic core is not necessarily zero (see fig. 4). Equations (46) and (51) would not, in this case, strictly apply. Saturation of the core will lead directly to degraded performance. A nonzero magnetic intensity drop around paths 2A, 3A, and 3B will also lead to degraded performance since the required excitation ampere-turns (NI) will be larger, resulting in larger coil electrical losses. To calculate B_c would therefore be interesting in order to determine for a given pump configuration if any of these effects are important.

The dimensionless core magnetic flux density β (see eq. (68)) is shown in figure 8 as a function of frequency magnetic Reynolds number $Re_{m\omega}$ for several values of the flow magnetic Reynolds number Re_{mv}. The curves for pump B are terminated at the point where $(Re_{m\omega}) = \left(Re^*_{m\omega}\right)_{min}$.

The section Ideal Quantities showed that for pump A the dimensionless pressure rise $\Delta\bar{p}_{id}$ was equal to 1 for all flow and frequency magnetic Reynolds numbers $Re^*_{m\omega}$ and Re_{mv}. Since both Δp_{id} and β are nondimensionalized with reference to excitation ampere-turns (NI), β gives a direct measure of the magnitude of B_c for a required value of Δp_{id}. Figure 8 shows that β becomes large as $Re_{m\omega}$ becomes small. An approximate expression for small $Re_{m\omega}$ can be obtained by combining equations (51), (68), and (116):

$$\beta \cong \left(\frac{2}{\pi}\right) \frac{Re_{mv}}{Re_{m\omega}\left(1 - e^{-Re_{mv}}\right)} \tag{121}$$

From equation (121), β increases with increasing Re_{mv} and decreases with $Re_{m\omega}$. From this it can be inferred that for low frequency excitation a very large core flux density B_c is required. (At $\omega = 0$, equation (121) gives $\beta = \infty$. This result is to be expected since a time-independent magnetic field should be incapable of producing a force

unless its strength is infinite.) For small values of $Re_{m\omega}$, then, figures 5, 6, and 7 and all those to be presented hereinafter may not be valid. Whether they are sufficient to describe any particular single-phase pump will depend on the permeability of the magnetic core material, its saturation flux density, and the particular geometrical characteristics of the pump. For most single-phase pump designs, the method and curves presented herein should be sufficient to describe the performance. An example of the use of these curves to design a lithium radiator coolant pump is given in appendix C.

COMPARISON WITH TRAVELING-FIELD PUMPS

Because the single-phase pump is an induction pump, comparison of its performance with that of a traveling-field induction pump of similar geometry and operating characteristics is interesting. The analysis that will be used for computations of traveling-field pump performance is reported in reference 4. This analysis includes effects of fluid and duct wall conductivities on the distribution and magnitude of the two-dimensional magnetic field. Allowances are also made for viscous losses and coil electrical losses. The analysis is, however, restricted to many wavelength pumps and configurations for which only the first space and time harmonics of the magnetic field are important.

The analogy between single-phase and traveling-field pumps is depicted in figure 9. The items that are compared are given in table I.

The wavelength λ in the traveling-field pump is made twice as long as the annulus length C in the single-phase pump because, over half a wavelength, the magnetic field in a traveling-field pump can be considered radially unidirectional. Since the magnetic field in the single-phase pump is radially unidirectional throughout the annulus C, the choice $\lambda = 2C$ provides a better analogy than $\lambda = C$.

The choice of a single coil width of $w/3$ in the traveling-field pump is based on the assumption of six coils per wavelength in this pump. Therefore, over half a wavelength, the total coil width is $3(w/3) = w$ and the total coil size is the same for both the single-phase and traveling-field pumps. If the coil current density j_e is the same for both, which is assumed, then the coil electrical losses are the same.

For the traveling-field pump, a dimensionless output pressure per wavelength $\Delta\bar{p}_\lambda$ is defined as follows:

$$\Delta\bar{p}_\lambda = \frac{1}{6}\left[\frac{2\,\Delta p_\lambda\left(r_{f,o}^2 - r_{f,i}^2\right)\ln\left(\frac{r_{f,o}}{r_{f,i}}\right)}{\mu\left(NI_\lambda\right)^2}\right] \tag{122}$$

where Δp_λ is the output pressure over one wavelength and NI_λ is the peak ampere-turns per single coil. Equation (122) is to be contrasted with equation (98) for $\Delta\bar{p}_{id}$ of the single-phase pump. If $\Delta\bar{p}_\lambda$ is defined as it was in equation (122), comparisons of $\Delta\bar{p}_\lambda$ and $\Delta\bar{p}_{id}$ indicate the relative magnitudes of the output pressure developed for a given amount of coil loss. The factor 1/6 in equation (122) is necessary since the quantity $(NI_\lambda)^2/2$ is proportional to the electrical loss in one coil only. In the traveling-field pump three-phase excitation and six coils per wavelength are assumed; hence, the total coil loss is proportional to $6(NI_\lambda)^2/2$.

Since the traveling-field pump analysis used allows two-dimensional effects to be included, $\Delta\bar{p}_\lambda$ as defined in equation (122) is not simply a function of $Re_{m\omega}$ and Re_{mv} as was the case for the single-phase pump, and if comparisons of $\Delta\bar{p}_{id}$ and $\Delta\bar{p}_\lambda$ are to be made, a particular geometry for the traveling-field pump is necessary. The geometry to be chosen will be that of the example given in appendix C; namely,

$$r_{f,i} = 0.04575 \text{ m}$$

$$r_{f,o} = 0.0491 \text{ m}$$

$$\lambda = 2C = 0.174 \text{ m}$$

Flow and frequency magnetic Reynolds numbers for a traveling-field pump will be taken so that

$$Re_{mv} = \mu\sigma vC = \mu\sigma v\frac{\lambda}{2} \tag{123}$$

and

$$Re_{m\omega} = \mu\sigma\left(\frac{C\omega}{\pi}\right)C = \mu\sigma\left(\frac{\lambda\omega}{2\pi}\right)\frac{\lambda}{2} \tag{124}$$

From these equations, the slip S, defined as

$$S = \frac{\text{Field speed - Fluid speed}}{\text{Field speed}} = \frac{\left(\frac{\lambda\omega}{2\pi}\right) - v}{\left(\frac{\lambda\omega}{2\pi}\right)} \tag{125}$$

is given by

$$S = \frac{Re_{m\omega} - Re_{mv}}{Re_{m\omega}} \tag{126}$$

Thus, the ideal efficiency of the traveling-field pump is

$$\left(\eta_{TF}\right)_{id} = 100(1 - S) = 100\left(\frac{Re_{mv}}{Re_{m\omega}}\right) \tag{127}$$

This function is plotted in figure 10 for the assumed value of Re_{mv} of 2.

The quantities $\Delta\bar{p}_{id}$ and $\Delta\bar{p}_{\lambda}$ are plotted in figure 11 for both single-phase and the assumed traveling-field pump configurations. Note that $\Delta\bar{p}_{\lambda}$ reaches a peak at some value of $Re_{m\omega}$ and then decreases, whereas $\left(\Delta p_{id}\right)_A$ stays constant and $\left(\Delta\bar{p}_{id}\right)_B$ increases with increasing $Re_{m\omega}$. The drop in $\Delta\bar{p}_{\lambda}$ at high values of $Re_{m\omega}$ has been predicted and experimentally verified in reference 5 for rotating-field devices. This drop is due to the fact that at high values of $(Re_{m\omega} - Re_{mv})$, magnetic field lines close by way of paths that are primarily in the flow direction. The body forces produced are therefore directed radially rather than axially. Furthermore, most of these field lines penetrate the surface of the fluid only (skin effect), which results in only a small net body force. For situations in which only high-frequency excitation is available, a single-phase pump might therefore be desirable because of this dropoff behavior of traveling-field pumps.

At high frequencies, efficiencies of single-phase pumps are, in general, greater than those of traveling-field pumps. Figure 10 shows curves of ideal and actual efficiency for traveling-field and single-phase pumps that satisfy the conditions outlined in appendix C. The curves for the ideal efficiencies of the single-phase pumps are obtained directly from figure 7(a). Each curve indicates how the efficiency of the particular pump it represents varies with frequency magnetic Reynolds number if the output pressure is fixed at the design value by varying the magnitude of the excitation ampere-turns.

The curves representing the single-phase pumps have been discussed previously. Curves of efficiency against $Re_{m\omega}$ are given for a traveling-field pump of four wavelengths. Comparisons of efficiencies of the four-wavelength traveling-field pump and the two single-phase pumps do not indicate that any one of these is substantially better for the application than any other. This conclusion is especially true if it is recalled that end effects have not been included in the traveling-field pump analysis and that a peak efficiency somewhat below that indicated in figure 10 will be the true efficiency. Further degradation in efficiency can also be expected because higher order space harmonics of the traveling field have not been included in the calculations.

A further inefficiency that may be present in the traveling-field pump results if the coils cannot be kept at the design temperature of 589° K without unreasonable amounts of cooling. If such is the case, then additional coil electrical losses can be expected because of increased resistivity of the coils. Cooling of the coils is, of course, also nec-

essary in the single-phase pump but primarily for removing the heat generated electrically within the coils themselves. Heat transfer from the hot fluid to the coils can be prevented by simply locating the coils far from the fluid and duct. This cannot be done in the traveling-field pump since the coils must be as close to the duct as possible to minimize leakage flux across the slots.

Another advantage of the single-phase pump configuration is that the electrical loss in the coils can be made insignificant by increasing the dimension w (see fig. 9). The coil loss for a required number of ampere turns NI are given by equation (82) by using $j_e = NI/hw$:

$$L_e = \frac{\pi}{2\sigma_e}\left(\frac{h + 2r_{e,i}}{h}\right)\frac{1}{w}(NI)^2 \tag{128}$$

Equation (128) shows that L_e can be made as small as desired by increasing w. In a single-phase pump this can be done easily. In a traveling-field pump, w cannot be made arbitrarily large or the higher order harmonics of the electromagnetic field produced will be sizeable. Also, if w is made too large the effective nonmagnetic gap is increased because of the large reluctance of the thin magnetic material between coils.

The coil loss L_e in a traveling-field pump can be reduced by increasing coil height h rather than width w; however, they cannot be made arbitrarily small. This can be seen by taking the limit of equation (128) as h becomes infinite while w remains fixed:

$$\lim_{h\to\infty} L_e = \frac{\pi}{2w\sigma_e}(NI)^2 \tag{129}$$

In actuality, it is doubtful that even this limit can be approached since the leakage flux across the coils is a factor whose importance increases with increasing h and thereby reduces the flux passing through the fluid.

A comparison of the weights of the selected angle-phase pump B and the most efficient four-wavelength traveling-field pump is desirable at this point. An approximation is sufficient and so the pump weight is assumed equal to the product of the weight density of the magnetic material (magnet steel density $\cong 8.01\times10^3$ kg/m^3, or 500 lb mass/ft^3) and the total pump volume. Since the coils are of copper, which has a density approximately equal to that of steel, the approximation should be quite close to the actual weight of the pump involved. In order to minimize the pump volume, all magnetic flux-carrying cross sections are assumed to have the same area and this area is sufficient to allow 10 000 gauss to pass. The result of such a calculation yields a single-phase pump B mass of 19.52 kilograms (43 lb) and a four-wavelength traveling-field pump mass of 34.50 kilograms (76 lb).

The design efficiencies, excitation frequencies, and masses of the single-phase pump B (see appendix C) and four-wavelength traveling-field pump therefore are as follows:

Single-phase pump B:

$$\eta = 13.8 \text{ percent}$$

$$\omega = 1096 \text{ rad/sec } (174.5 \text{ cps})$$

$$\text{mass} = 19.52 \text{ kg } (43 \text{ lb})$$

Four-wavelength traveling-field pump:

$$\eta = 16.0 \text{ percent}$$

$$\omega = 579 \text{ rad/sec } (92.2 \text{ cps})$$

$$\text{mass} = 34.5 \text{ kg } (76 \text{ lb})$$

SUMMARY OF RESULTS

Analyses of two types of single-phase induction pumps have been made and performance prediction methods have been outlined. Ideal and general performances of each have been discussed, and the following results have been obtained:

1. Performance of both single-phase electromagnetic pumps can be conveniently described in terms of a flow magnetic Reynolds number Re_{mv} and a frequency magnetic Reynolds number $Re_{m\omega}$. In the limit of very high values of $Re_{m\omega}$ and/or very low values of Re_{mv}, the performance of both pumps is the same.

2. Dimensionless quantities are defined from which calculations of the efficiency, magnetic core flux density, and voltage requirements of single-phase pumps can be made. Each of these dimensionless quantities is a function of both $Re_{m\omega}$ and Re_{mv}.

3. In the ideal case for which coil electrical, duct-wall electrical, and viscous losses are zero and only fluid electrical losses are included, the following conclusions can be made:

a. Pump A (low-reluctance path at outlet): For this case, the ideal output pressure is independent of both $Re^*_{m\omega}$ and Re^*_{mv} (asterisk refers to ideal quantities) and depends only on the annulus geometry and the magnitude of the excitation ampere-turns NI. The ideal efficiency decreases with $Re^*_{m\omega}$ and increases with Re^*_{mv}. The ideal efficiency at low values of Re^*_{mv} and $Re^*_{m\omega}$ can be shown to be approximately equal to 100 $(Re^*_{mv}/2)$, and the maximum value of the ideal efficiency is 50 percent. This

value is attained in the limit of zero $Re^*_{m\omega}$ and infinite Re^*_{mv}.

b. Pump B (no low-reluctance path at outlet): This pump exhibits a characteristic similar to that of traveling-field pumps. There exists a minimum value of $Re^*_{m\omega}$, referred to as $\left(Re^*_{m\omega}\right)_{min}$, below which pumping is not possible. The value of $\left(Re^*_{m\omega}\right)_{min}$ increases with increasing Re^*_{mv}. As $Re^*_{m\omega}$ is increased from $\left(Re^*_{m\omega}\right)_{min}$ at constant Re^*_{mv} and NI, the ideal output pressure increases and approaches asymptotically the corresponding value of pump A. Similarly, the ideal efficiency increases, reaches a peak, and then approaches the ideal efficiency of pump A for the same Re^*_{mv}.

4. Single-phase pumps A and B were designed for pumping lithium at 922° K (1200° F) at a volume flow rate of 10^{-2} cubic meters per second (158 gal/min) and an output pressure of 10^5 Newtons per square meter (14.5 lb/in.^{2}). By choosing maximum efficiency consistent with a maximum allowable core magnetic field strength, optimum efficiencies were found to be 14.1 percent for pump A and 13.8 percent for pump B. Because the difference of 0.3 percentage points is small and since pump B offers a simpler duct construction, pump B is probably better for the application.

5. Comparisons of single-phase and traveling-field induction pumps show the single-phase pump to be potentially competitive or superior in efficiency, reliability, and weight for the following applications:

a. High-temperature applications

b. High-flow, low-output-pressure applications

c. Situations in which only high-frequency excitation is available

Lewis Research Center,
National Aeronautics and Space Administration,
Cleveland, Ohio, November 18, 1966,
120-27-04-05-22.

APPENDIX A

SYMBOLS

A	area enclosed within path, m^2
a	radius of central magnetic core, m
B	magnetic field strength (without subscript implies radial component), WB/m^2
B_s	effective magnetic core flux density, Wb/m^2
b	complex function containing dependence of B_r on ζ, $Re_{m\omega}$, and Re_{mv}, dimensionless
C	annulus length, m
C_f	friction factor, dimensionless
C_0	integration constant, Wb/m^2
C_1, C_2	integration constants, Wb/m
E	electric field strength, V/m
E_{app}	electric field strength applied to conduction electromagnetic pump, V/m
E_i	electric field strength at annulus inlet
e	complex function containing dependence of E on ζ, $Re_{m\omega}$, and Re_{mv}, dimensionless
F	force produced by electromagnetic field, N
g	gap height in conduction electromagnetic pump, m
H	magnetic field intensity, A/m
h	radial coil height, m
I	electric current per coil turn, A
$\hat{i}$	unit vector in x-direction
j	electrical current density, A/m^2
K_1, K_2	complex constants, m (see eq. (46))
$\hat{k}$	unit vector in z-direction
L	power loss, W
l	dummy integration variable implying a differential portion of integration path, m
l_s	effective length of integration path in magnetic core, m
N	number of coil turns
NI	number of coil ampere-turns
$\mathcal{O}$	of the order of
P	path around which $\vec{H}$ is integrated
PFF	power factor function, dimensionless
$\mathscr{P}$	power input, W
Δp	pressure rise, N/m^2
Q	defined on p. 34, Wb^2/m
Q'	defined on p. 36, Wb^2/m
Re	Reynolds number, dimensionless

Re'_m, Re''_m	complex magnetic Reynolds numbers, dimensionless (defined on p. 12)
Re_{mv}	flow magnetic Reynolds number, dimensionless
$Re_{m\omega}$	frequency magnetic Reynolds number, dimensionless
$\mathscr{R}$	real part of
r	radial coordinate, m
$\hat{r}$	unit vector in r-direction
S	slip, dimensionless
t	time, sec
V	voltage across coil, V
V_s	negative of slip velocity, m/sec
v	velocity (without subscript implies fluid velocity), m/sec
v_s	slip velocity, m/sec
v_w	traveling field or wave velocity, m/sec
W	mechanical power, W
w	axial coil width, m
x	coordinate in direction of current flow in a conduction pump, m
y	coordinate in direction of magnetic field in a conduction pump, m
z	coordinate in direction of flow, m
z'	dummy integration variable, m
α	function containing dependence of radial magnetic field on z, Wb/m
α'	function containing dependence of radial magnetic field on z and r, Wb/m^2
β	magnetic core flux density, dimensionless
γ	function containing dependence of electric field on z, V
γ'	function containing dependence of electric field on z and r, V/m
ϵ	a number much less than 1
ζ	dimensionless axial coordinate, z/C
η	efficiency, dimensionless
θ	circumferential coordinate, rad
$\hat{\theta}$	unit vector in θ-direction
λ	wavelength of traveling-field pump, m
μ	permeability (without subscript implies permeability of free space), H/m
μ_f	absolute viscosity of pumped fluid, $N\text{-}sec/m^2$
ρ	mass density, kg/m^3
σ	electrical conductivity, $(ohm/m)^{-1}$

τ	dummy volume integration variable, m^3
φ, χ, ψ	dimensionless functions defined in equations (59), (60), and (61)
φ_m	magnetic flux, Wb
φ_v	potential voltage, V
ω	frequency of excitation, rad/sec

Subscripts:

A	pump A
B	pump B
c	central magnetic core
e	exciting coils
f	pumped fluid
H	viscous losses
I	imaginary component of
i	for annulus, implies inner fluid radius; for coil, implies inside radius
id	ideal
j	pertaining to j^{th} coil turn
k	pertaining to k^{th} medium in annulus
m	pertaining to electromagnetic field
min	minimum value
n	largest value for k
o	for annulus, implies outer fluid radius; for coil, implies outside radius
R	real component of
r	component in r-direction
rms	root-mean-square value
TF	traveling-field pump
t	pertaining to one coil turn
y	component in y-direction
λ	value over one wavelength of traveling-field pump
θ	component in θ-direction

Superscripts:

$\rightarrow$	vector quantity
*	defined for case where only fluid exists in annulus
–	dimensionless

APPENDIX B

ELECTROMAGNETIC BODY FORCE $\vec{F}$ AS DIFFERENCE BETWEEN INLET AND OUTLET MAGNETIC PRESSURES WHEN ELECTRIC FIELD $\vec{E}_{app}$ IS APPLIED

In the conduction electromagnetic pump $B_y^2(0)$ is made greater than $B_y^2(C)$ by the application of an electric field $\vec{E}_{app}$ in the positive x-direction. If all previous assumptions are made and $\vec{E}_{app}$ is assumed constant, equations (2) and (5) imply that

$$\frac{1}{\mu}\frac{\partial B_y}{\partial z} = \sigma(vB_y - E_{app}) \tag{B1}$$

Equation (B1) is solved by

$$B_y = \frac{E_{app}}{v} + C_0 e^{\mu\sigma vz} \tag{B2}$$

Requiring again that

$$\varphi_m = \int_0^C B_y \, dz$$

implies that

$$C_0 = \frac{\mu\sigma v\left(\varphi_m - E_{app}\frac{C}{v}\right)}{e^{\mu\sigma vC} - 1} \tag{B3}$$

and

$$B_y = \frac{E_{app}}{v} - \frac{E_{app}}{v}\left(\frac{\mu\sigma vC}{e^{\mu\sigma vC} - 1}\right)\left(1 - \frac{\varphi_m v}{E_{app}C}\right)e^{\mu\sigma vz} \tag{B4}$$

Now

$$0 \le \frac{\mu\sigma vC}{e^{\mu\sigma vC} - 1} \le 1$$

For pumping operation, E_{app} is made large enough to ensure that

$$0 \leq \frac{\varphi_m v}{E_0 C} < 1$$

Therefore,

$$0 < \left(\frac{\mu\sigma vC}{e^{\mu\sigma vC} - 1}\right)\left(1 - \frac{\varphi_m v}{E_{app} C}\right) = K < 1$$

under normal circumstances. Equation (17) can be written

$$B_y = \frac{E_{app}}{v}(1 - Ke^{\mu\sigma vz}) \tag{B5}$$

Applying the condition $B_y^2(0) > B_y^2(C)$ results in a fairly complex relation of K and the flow magnetic Reynolds number $Re_{mv} = \mu\sigma vC$. For reasonable values of K and Re_{mv} this condition can usually be satisfied. The situation for which $E_{app}/v = 2$ webers per square meter, $K = 1/2$, and $Re_{mv} = \ln 2$ is depicted in figure 1(b). In this case $B_y^2(0) = 1\ (Wb/m^2)^2$ and $B_y^2(C) = 0\ (Wb/m^2)^2$, resulting in a positive pumping force (see fig. 12).

APPENDIX C

USE OF ANALYSIS AND RESULTANT CURVES FOR CALCULATING DESIGN AND PERFORMANCE OF PARTICULAR PUMP APPLICATION

Figures 13, 14, and 15 give the dimensionless quantities φ, χ, and ψ as functions of frequency magnetic Reynolds number at several values of flow magnetic Reynolds number. These curves along with the dimensionless core flux density β (fig. 8) and the power factor function PFF (fig. 16) are sufficient to enable calculations of performance to be made with relative ease.

Consider the single-phase induction pump as the pumping unit for a lithium radiator coolant application and further assume that the required operating conditions are as follows:

Operating temperature = 922° K (1200° F)

Output pressure = 10^5 N/m^2 (14.5 psi)

Volume flow rate = 10^{-2} m^3/sec (158 gal/min)

Fluid velocity = 10 m/sec (32.8 ft/sec)

Duct wall material = tantalum T-111 at 922° K

Coils = Copper at 589° K (600° F)

Current density = 10^7 A/m^2

Core magnetic field strength = $B_c \leq 1.5$ Wb/m^2

If it is assumed that only the pumped fluid, lithium, and two tantalum duct walls (see fig. 3) exist in the annulus, then subscripts 1 and 3 refer to the duct walls, and the subscript 2 refers to the fluid. The important properties of the fluid and duct walls at 922° K are as follows:

$$\sigma_2 = 2.57 \times 10^6 \text{ (ohm-m)}^{-1}$$

$$\rho_2 = 470 \text{ kg/m}^3 \text{ (29.5 lb/ft}^3\text{)}$$

$$\mu_{f,2} = 2.975 \times 10^{-4} \text{ N-sec/m}^2 \text{ (2} \times 10^{-4} \text{ lb mass/ft-sec)}$$

$$\sigma_1 = \sigma_3 = 2.07\times10^6 \text{ (ohm-m)}^{-1}$$

and the conductivity of copper at 589° K is

$$\sigma_e = 29.7\times10^6 \text{ (ohm-m)}^{-1}$$

Further assume a duct-wall thickness of 0.00075 meter (0.03 in.) and the following values of a, r_1, r_2, and w

$$a = 0.04 \text{ m } (1.587 \text{ in.})$$

$$r_1 = 0.045 \text{ m } (1.786 \text{ in.})$$

$$r_2 = 0.04575 \text{ m } (1.816 \text{ in.})$$

$$w = 0.03 \text{ m } (0.01181 \text{ in.})$$

Since the fluid velocity v_2 is given as an input at 10 meters per second, the value of r_3 can be obtained from

$$\pi\left(r_3^3 - r_2^2\right)v_2 = \text{Volume flow rate}$$

Since the volume flow rate is 10^{-2} cubic meter per second, it follows that

$$\pi\left[r_3^2 - (0.04575)^2\right]10 = 10^{-2}$$

Solving for r_3 in this equation yields

$$r_3 = 0.0491 \text{ m } (1.948 \text{ in.})$$

$$r_4 = r_3 + w = 0.04985 \text{ m } (1.978 \text{ in.})$$

In order to determine the length C the flow magnetic Reynolds number Re_{mv} at which to operate must be specified. Figure 7 shows that if Re_{mv} is too small, the efficiency will be low. If Re_{mv} is chosen too high, B_c may be too high (refer to the discussion in the previous section). As a compromise choose

$$Re_{mv} = 2$$

If $\mu = 4\pi \times 10^{-7}$ henry per meter (permeability of free space), the required length C can be computed from equation (33):

$$2 = C\left[\frac{4\pi(10^{-7})}{\ln\left(\frac{4.985}{4.5}\right)} 2.57(10^{6})(10)\ln\left(\frac{4.91}{4.575}\right)\right]$$

or

$$C = 0.087 \text{ m } (3.452 \text{ in.})$$

Since figure 7 indicates that pump A always has a higher ideal efficiency than pump B, pump A is the pump under consideration for this particular calculation. The value of $Re_{m\omega}$ must now be chosen for pump A. If $Re_{m\omega}$ is chosen too high, the efficiency will be low. If $Re_{m\omega}$ is chosen too low, a value of B_c that is not permissible may be obtained. From figure 7, a reasonable value of $Re_{m\omega}$ seems to be 6.

Using the computed value of C, the required excitation frequency can now be obtained from equation (34). The result is

$$\omega = 822 \text{ rad/sec} = 131 \text{ cps}$$

At an Re_{mv} value of 2 and an $Re_{m\omega}$ value of 6, figures 8, 13, 14, and 15 give

$$\beta = 0.550$$

$$\varphi = 0.057$$

$$\chi = 0.170$$

$$\psi = 0.770$$

The required output power W can be computed from the values of output pressure and flow rate given as inputs:

$$W = (\text{output pressure})(\text{flow rate})$$

$$= (10^{5})(10^{-2})$$

$$= 1000 \text{ W}$$

Since the net output power W is the difference between the work done by the electromagnetic field W_m and the viscous losses L_H, L_H must first be computed in order to get the required value of W_m. The Reynolds number Re_2 is obtained from equation (84):

$$Re_2 = \frac{2(470)10(0.0491 - 0.04575)}{2.975(10^{-4})}$$

$$= 1.06\times10^5$$

Using equation (86) gives a value for $C_{f,2}$ of 0.0175. With this value equations (87) and (88) give

$$L_{H,2} = L_H$$

$$= 170 \text{ W}$$

Therefore,

$$W_m = L_H + W$$

$$= 1000 + 170$$

$$= 1170 \text{ W}$$

The required value of B_c can now be obtained from equation (62). The result of this calculation is a value for B_c of 1.247 webers per square meter, which is within the limit $B_c \leq 1.5$ webers per square meter. Using this value of B_c in equation (63) gives the total electrical losses L_m in the annulus of 5908 watts.

The required value of NI is obtained from equation (73) for $\beta = 0.550$. The result is $NI = 3350$ ampere-turns (peak value).

Assuming a coil width w of 0.03 meter (1.191 in.) and recalling that the required coil current density j_e is 10^7 amperes per square meter allows the necessary coil height h to be computed from

$$h = \frac{NI}{j_e w}$$

$$= \frac{3350}{10^7\ 3(10^{-2})}$$

$$\cong 1.12\times10^{-2} \text{ m } (0.438 \text{ in.})$$

If the minimum coil radius $r_{e,i}$ is made to be the same as the radius a of the low-radius portion of the core, then the maximum radius of the coil $r_{e,o}$ is

$$r_{e,o} = r_{e,i} + h$$

$$= 0.04 + 0.0112$$

$$= 0.0512 \text{ m } (2.025 \text{ in.})$$

Using equation (82) to compute the coil losses results in $L_e = 162$ watts. The total input power $\mathscr{P}$ is the sum of W_m, L_m, and L_e:

$$\mathscr{P} = W_m + L_m + L_e$$

$$= 1170 + 5908 + 162$$

$$= 7340 \text{ W}$$

The efficiency η is therefore

$$\eta = \frac{W}{\mathscr{P}} 100$$

$$= \frac{1000}{7240} 100$$

$$= 13.8 \text{ percent}$$

This value of efficiency, of course, is not necessarily the best obtainable under the conditions of operation imposed. Better efficiencies could conceivably be obtained at higher or lower values of the flow and frequency magnetic Reynolds numbers. Other parameters such as fluid velocity and dimensions might also be varied. Figure 10 shows how efficiency varies with $Re_{m\omega}$ if the values of Re_{mv}, j_e, w, a, r_1, r_2, r_3, r_4, and C are held fixed. This is done for both pumps A and B for the volume flow rate of 10^{-2} cubic meter per second and output pressure of 10^5 newtons per square meter. The efficiency of pump A remains relatively constant to a frequency magnetic Reynolds number of approximately 7 and decreases with $Re_{m\omega}$ slowly. The section Magnetic Flux Density Considerations showed that, for very low values of $Re_{m\omega}$, the necessary value of B_c for a given output pressure and flow is large. Therefore, the selection of a pump operating frequency will be based on maximum efficiency consistent with an inner core field strength B_c which is less than or equal to 1.5 webers per square meter.

Figure 17 shows how the required value of B_c varies with $Re_{m\omega}$ for both pumps A and B. For pump A, the lowest permissible value of $Re_{m\omega}$ is approximately 4.65, whereas for pump B, $Re_{m\omega} \cong 5.375$ is the minimum value. At the $Re_{m\omega}$ value of 4.65, figure 10 gives an efficiency for pump A of approximately 14.1 percent. Since efficiency decreases as $Re_{m\omega}$ increases, this represents the best efficiency obtainable in pump A for the particular conditions considered. For pump B, however, the best efficiency is not obtained at the point where $B_c = 1.5$ webers per square meter, but peaks at an $Re_{m\omega}$ value of approximately 8. At this value of $Re_{m\omega}$ the efficiency is approximately 13.8 percent, and B_c is approximately 1 weber per square meter. The efficiencies, required excitation frequencies, and required core magnetic field strengths B_c for pumps A and B at design conditions are therefore:

Pump A:

$$\eta = 14.1 \text{ percent}$$

$$\omega = 637 \text{ rad/sec} = 101.3 \text{ cps}$$

$$B_c = 1.5 \text{ Wb/m}^2$$

Pump B:

$$\eta = 13.8 \text{ percent}$$

$$\omega = 1096 \text{ rad/sec} = 174.5 \text{ cps}$$

$$B_c = 1.0 \text{ Wb/m}^2$$

Therefore, for the particular application considered and for an Re_{mv} of 2, the optimum efficiencies of pumps A and B are not greatly different. Since pump B offers a simpler hydraulic design, this pump would probably be chosen and the 0.3 percentage points difference in efficiency sacrificed.

REFERENCES

1. Verkamp, J. P.; and Rhudy, R. G.: Electromagnetic Alkali-Metal Pump Research Program. NASA CR-380, 1966.

2. Watt, D. A.: A Single Phase Annular Induction Pump for Liquid Metals. Rep. No. AERE-ED/R-1844, Atomic Energy Research Establishment, Great Britain, Jan. 21, 1953. (Declassified version of AERE-CE/R-1090.)

3. Vennard, J. K.: Elementary Fluid Mechanics. John Wiley & Sons, Inc., 1947, pp. 157-161.

4. Schwirian, Richard E.: Analysis of Linear-Induction or Traveling-Wave Electromagnetic Pump of Annular Design. NASA TN D-2816, 1965.

5. Schwirian, Richard E.: Effect of Magnetic Reynolds Number in Rotating MHD Induction Machines. M. S. Thesis, Case Institute of Technology, 1964.

TABLE I. - COMPARISON OF SINGLE-PHASE AND TRAVELING-FIELD PUMPS

Dimensions and conditions	Pump	
	Single-phase	Traveling-field
Fluid temperature, ^{o}K	922	922
Coil temperature, ^{o}K	589	589
Annulus length	C	1/2 wavelength λ
Inner fluid radius	$r_{f,i}$	$r_{f,i}$
Outer fluid radius	$r_{f,o}$	$f_{f,o}$
Coil height	h	h
Coil width	w	w/3
Coil current density	j_e	j_e
Flow magnetic Reynolds number	2	2

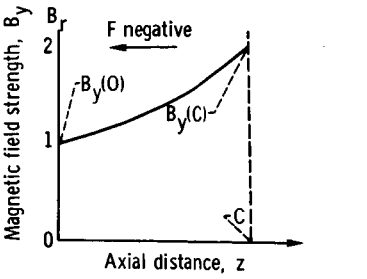

(a) Magnetic field strength as function of axial distance.

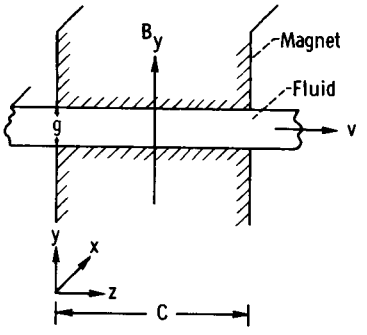

(b) Magnet-fluid geometry.

Figure 1. - Relation of magnetic field distribution to electromagnetic body force (without electric field).

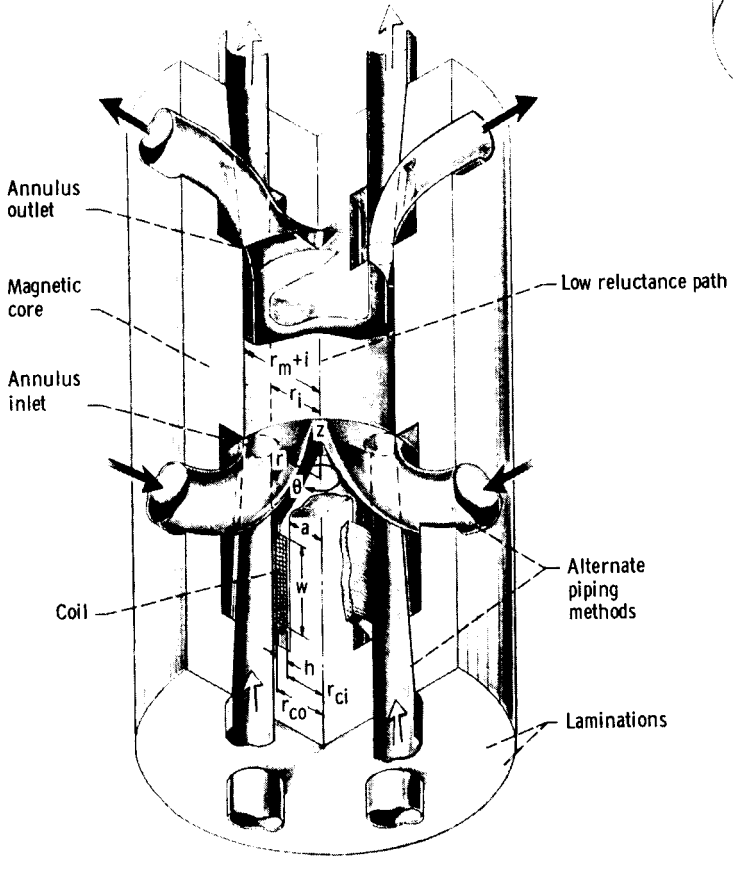

(a) Pump A, zero magnetic field outlet.

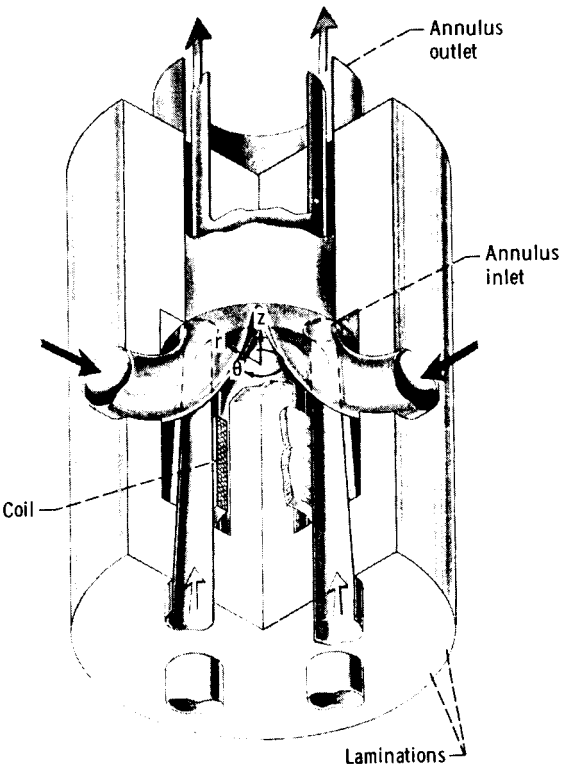

(b) Pump B, zero electric field outlet.

CD-8779

Figure 2. - Single-phase pump configurations.

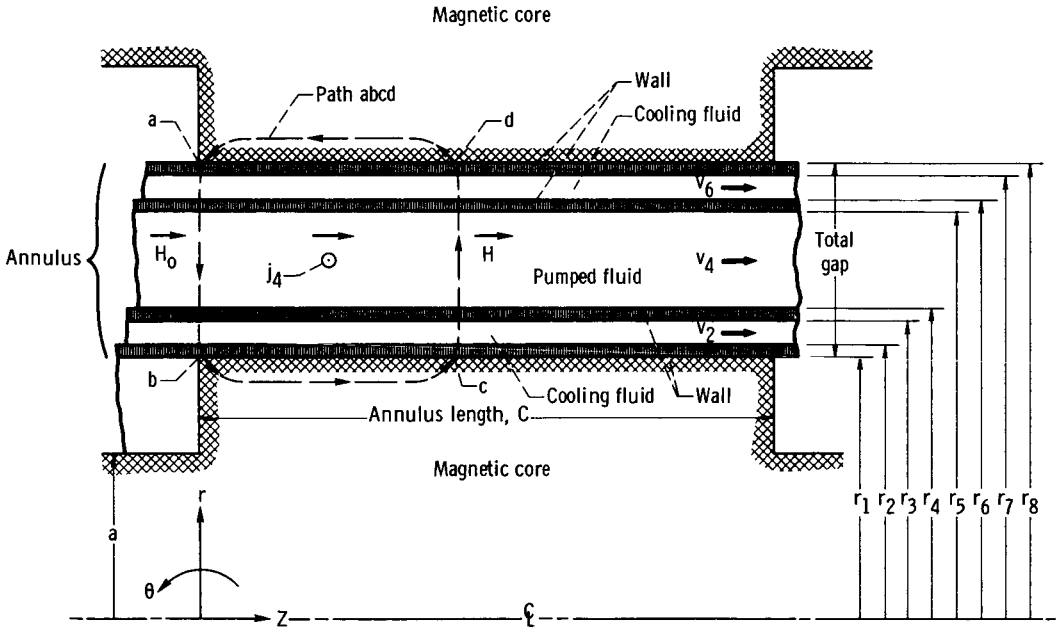

Figure 3. - Analytical model of annulus.

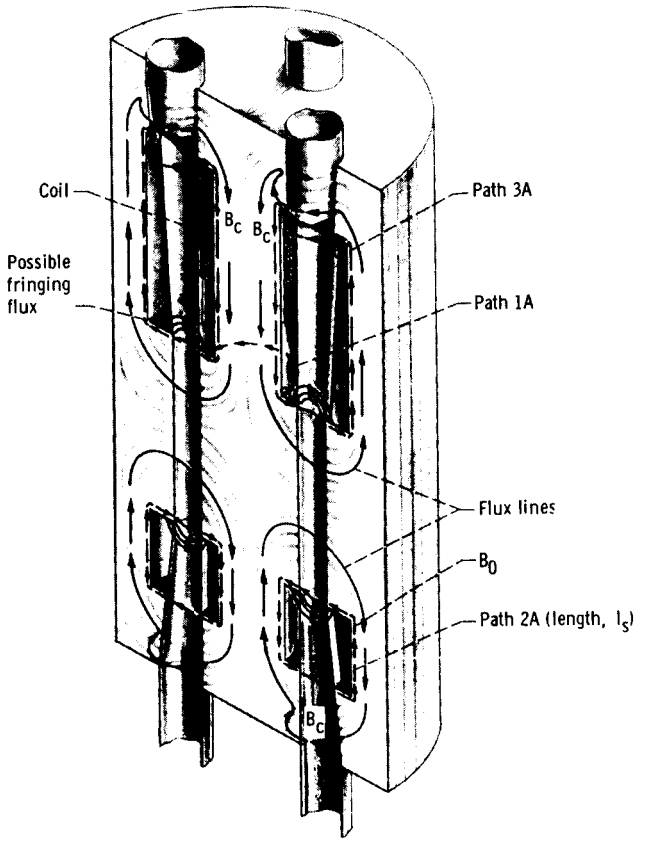

(a) Pump A, zero magnetic field outlet.

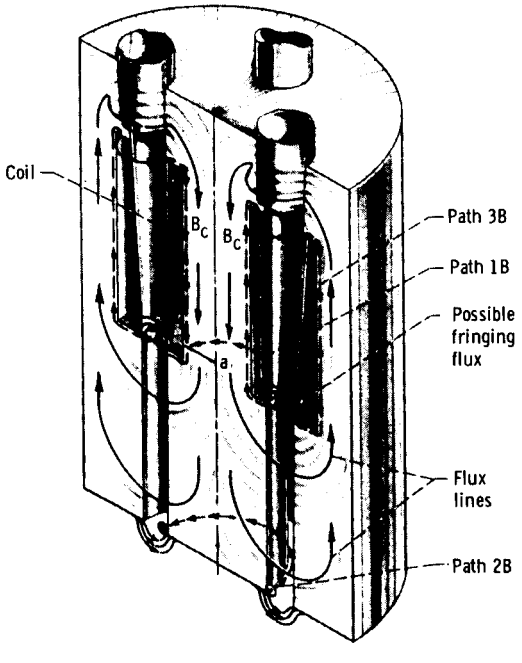

(b) Pump B, zero electric field outlet.

CD-8778

Figure 4. - Derivation of boundary conditions.

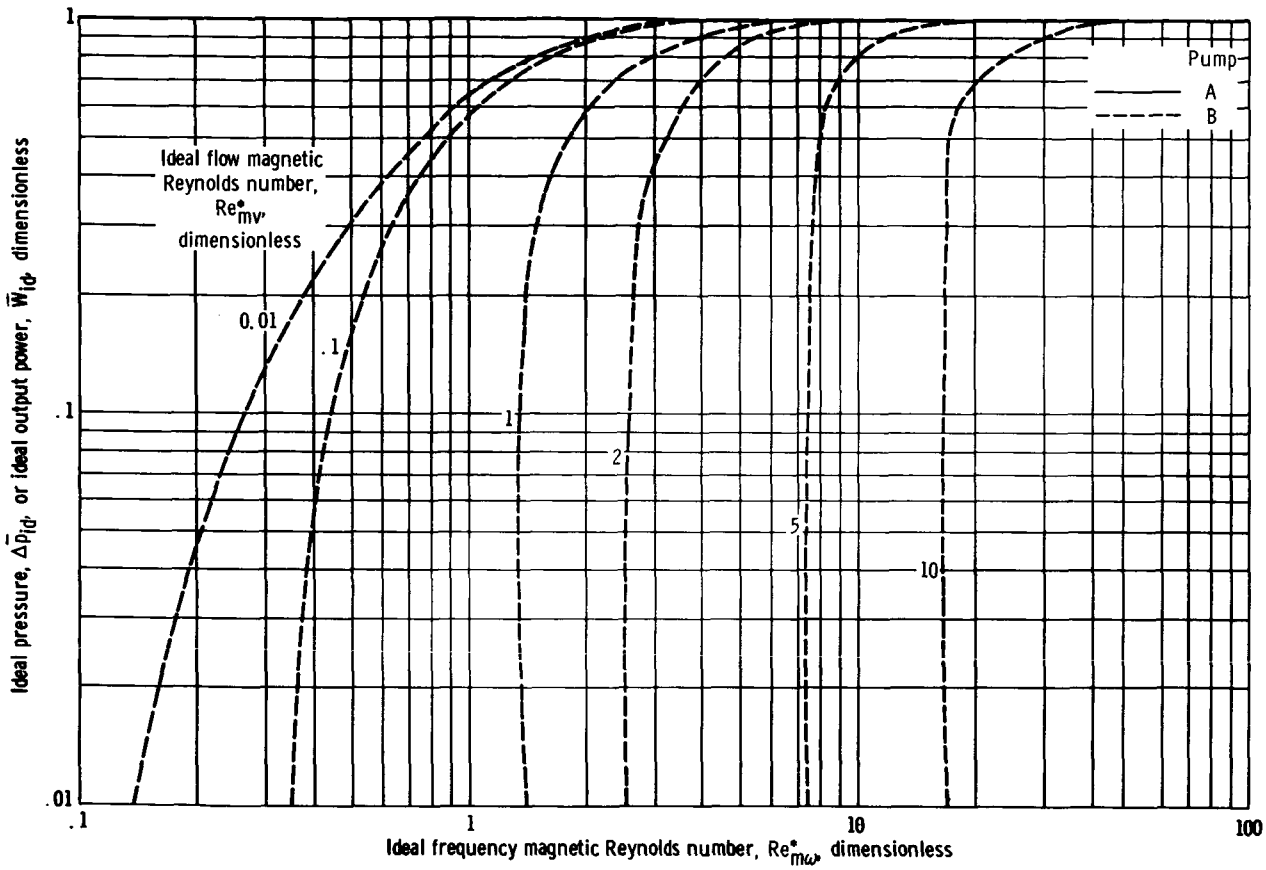

(a) Variation of dimensionless ideal pressure, or output power, with ideal frequency magnetic Reynolds number.

Figure 5. - Dimensionless ideal pressure, or output power, for single-phase induction pumps of zero magnetic field and zero electric field outlet.

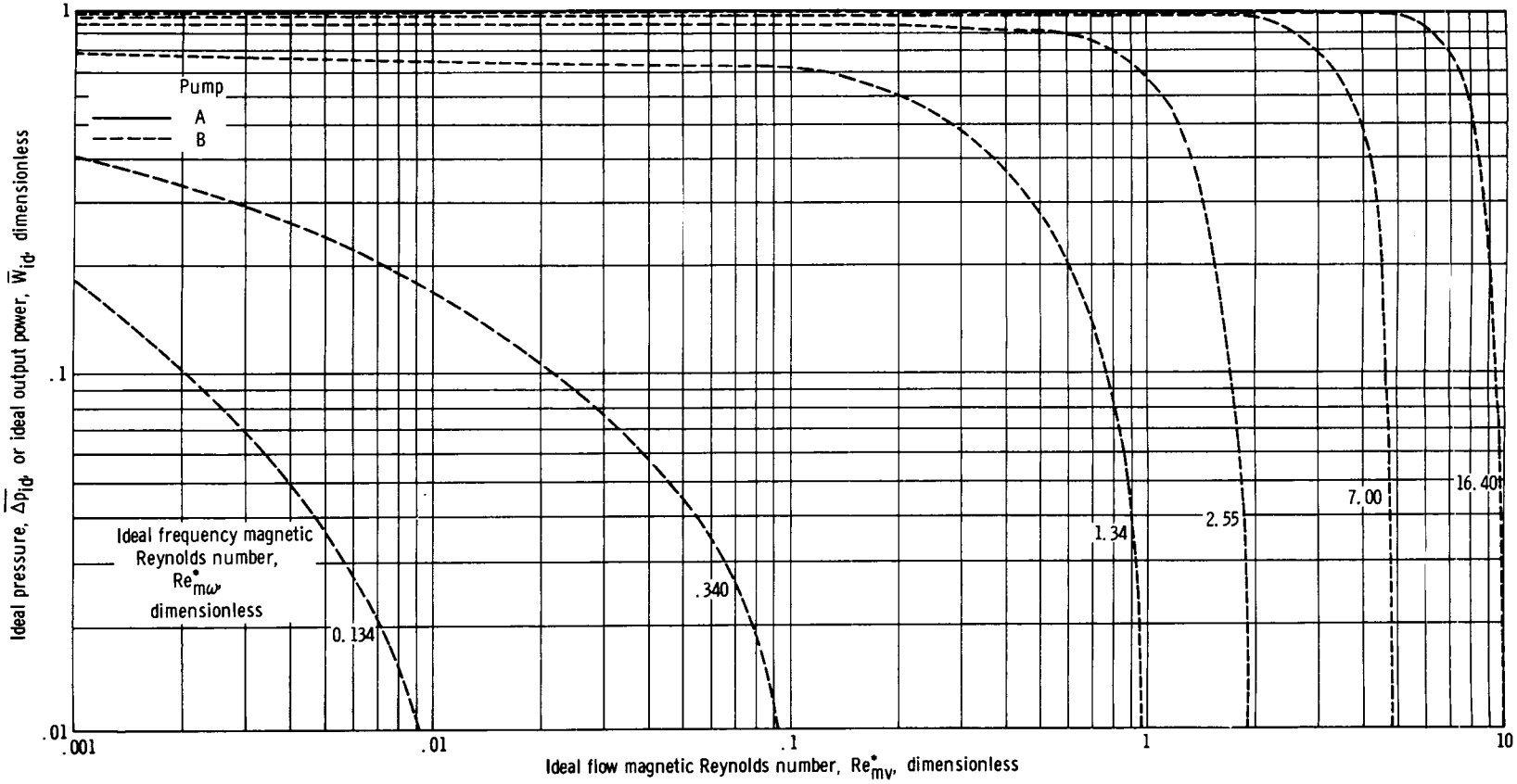

(b) Variation of dimensionless ideal pressure, or output power, with ideal flow magnetic Reynolds number.

Figure 5. - Concluded.

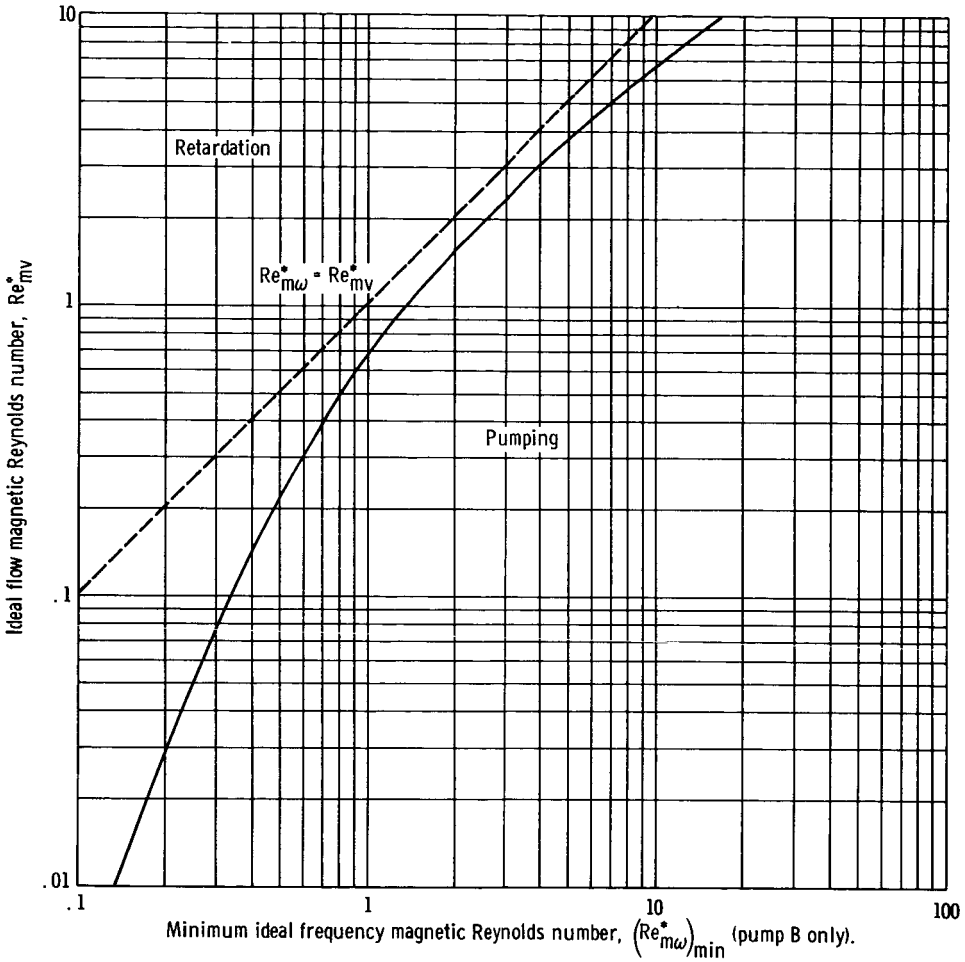

Figure 6. - Variation of ideal flow magnetic Reynolds number with minimum ideal frequency magnetic Reynolds number.

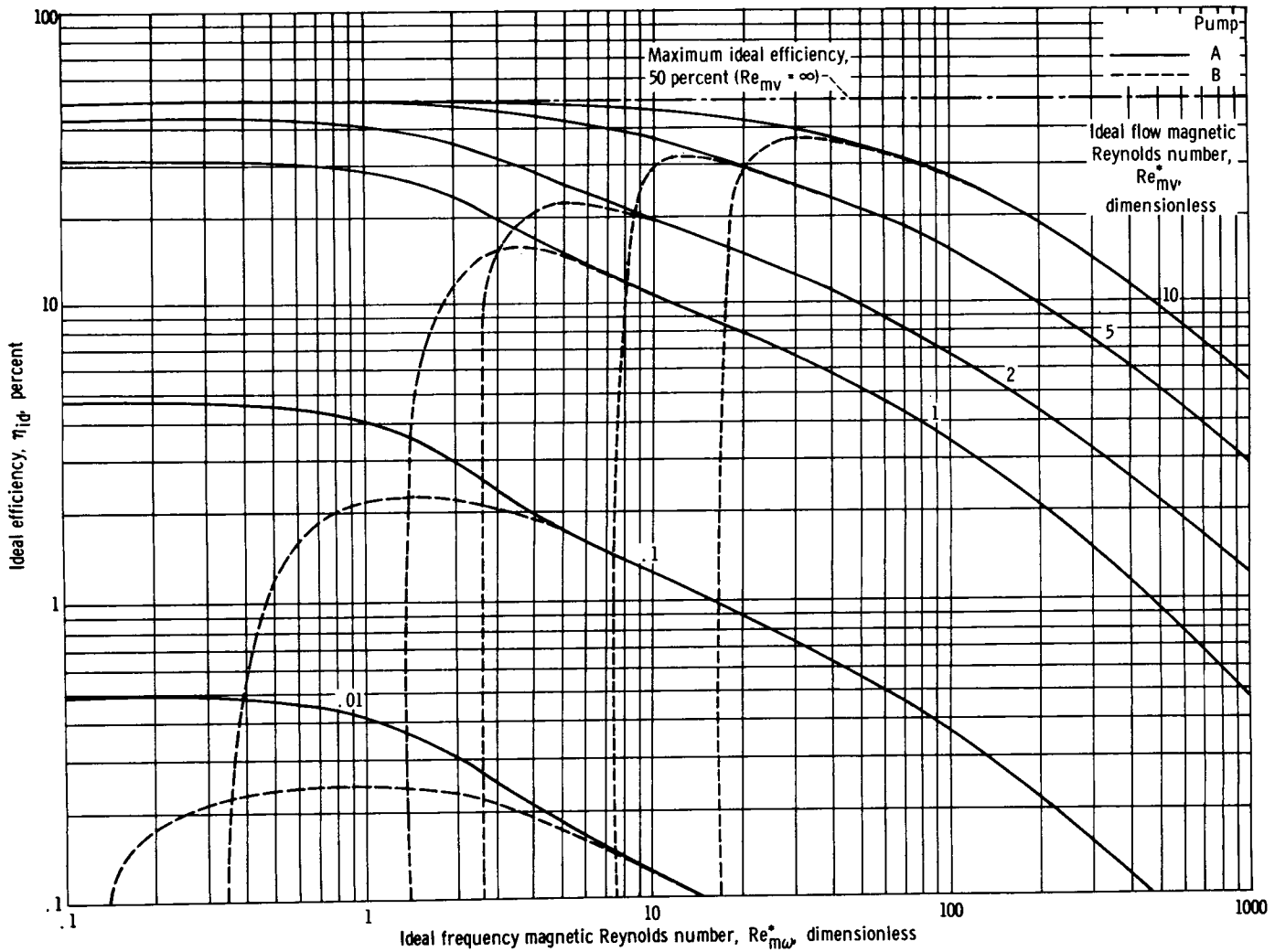

(a) Variation of ideal efficiency with ideal frequency magnetic Reynolds number at several values of ideal flow magnetic Reynolds number.

Figure 7. - Ideal efficiency of single-phase induction pumps of zero magnetic field and zero electric field (pumps A and B).

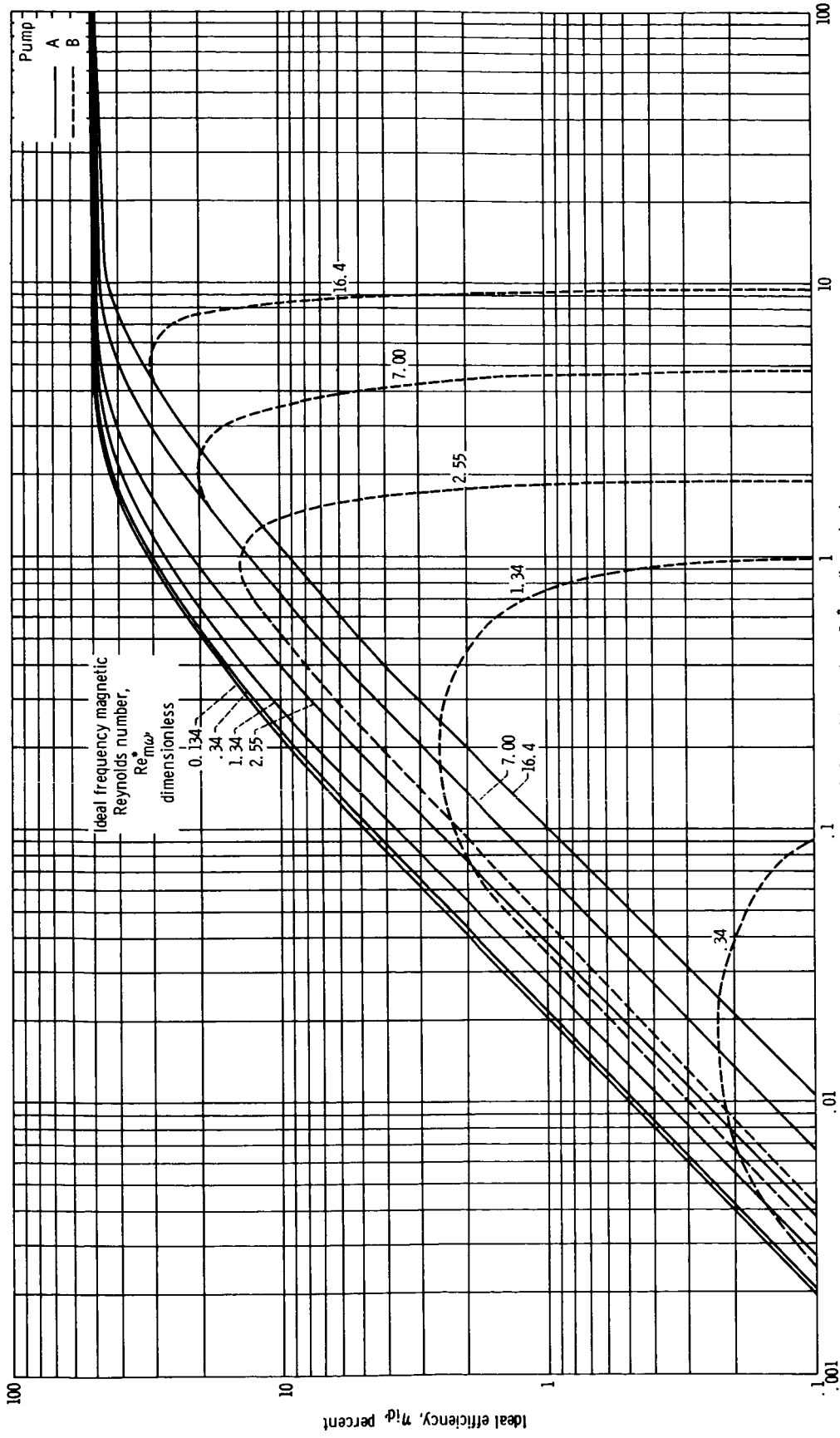

(b) Variation of ideal efficiency with ideal flow magnetic Reynolds number at several values of frequency magnetic Reynolds number.

Figure 7. - Concluded.

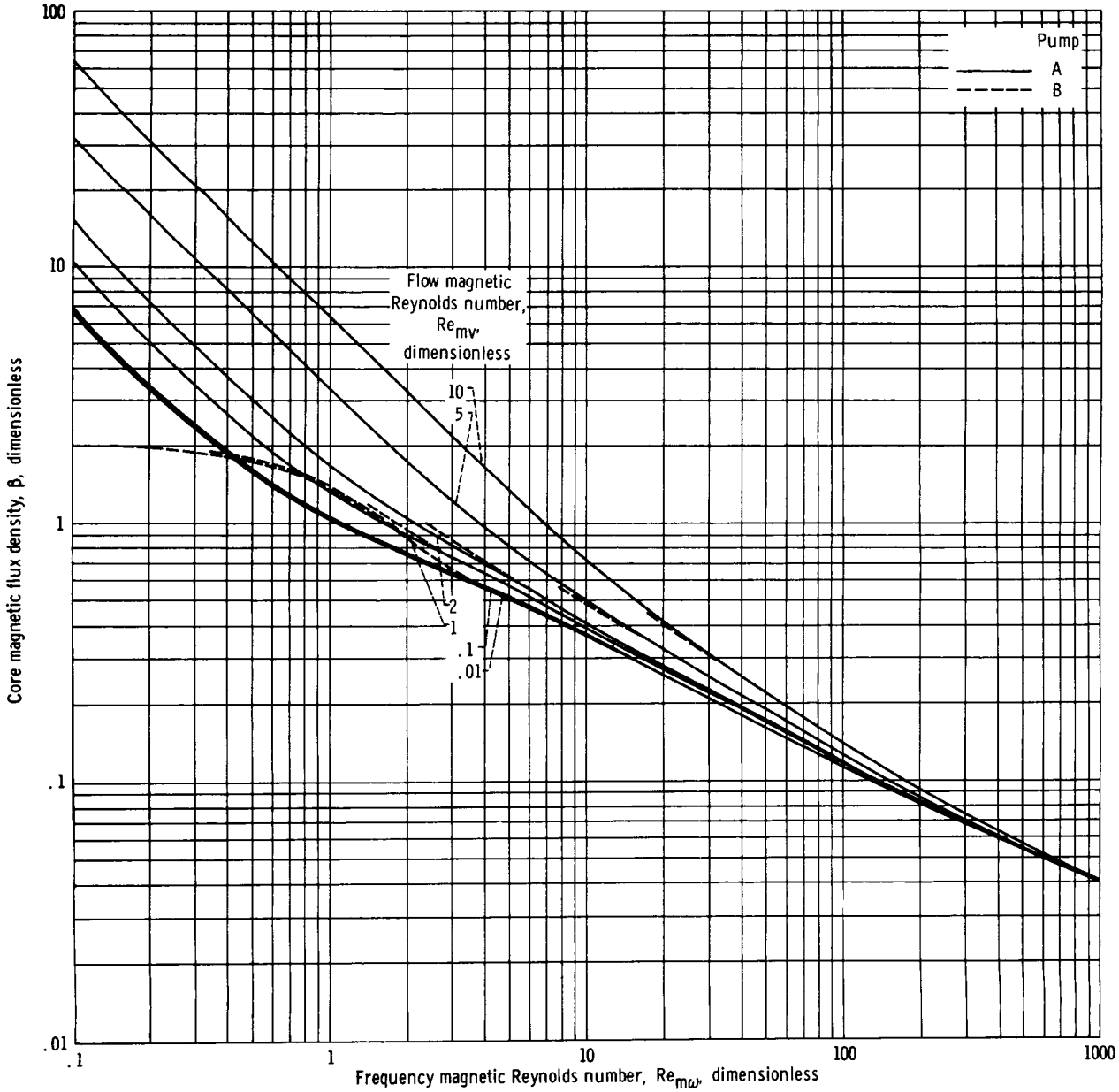

Figure 8. - Dimensionless core magnetic flux density of single-phase induction pumps A and B with zero magnetic field and zero electric field outlet.

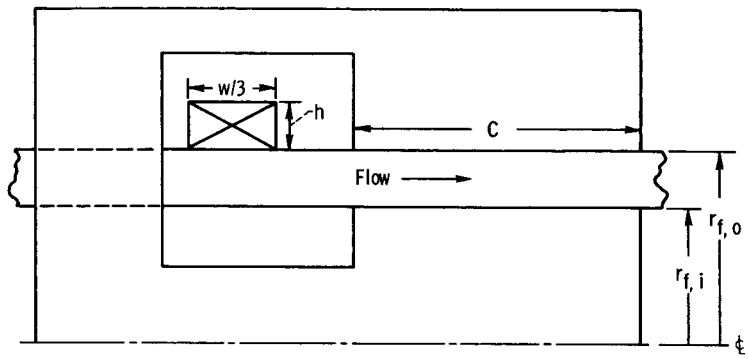

(a) Single-phase pump configuration.

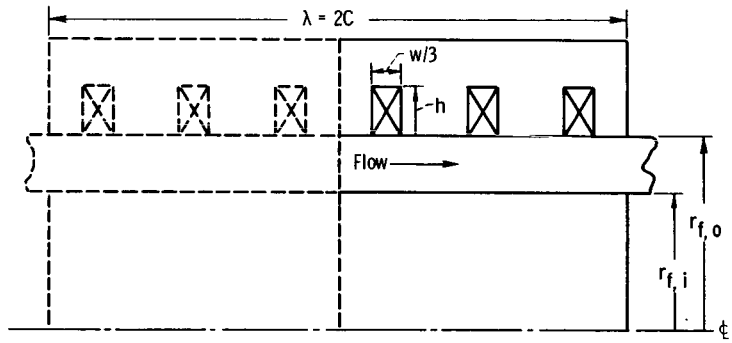

(b) Similar traveling-field pump configuration.

Figure 9. - Comparison of single-phase and traveling-field electromagnetic pumps.

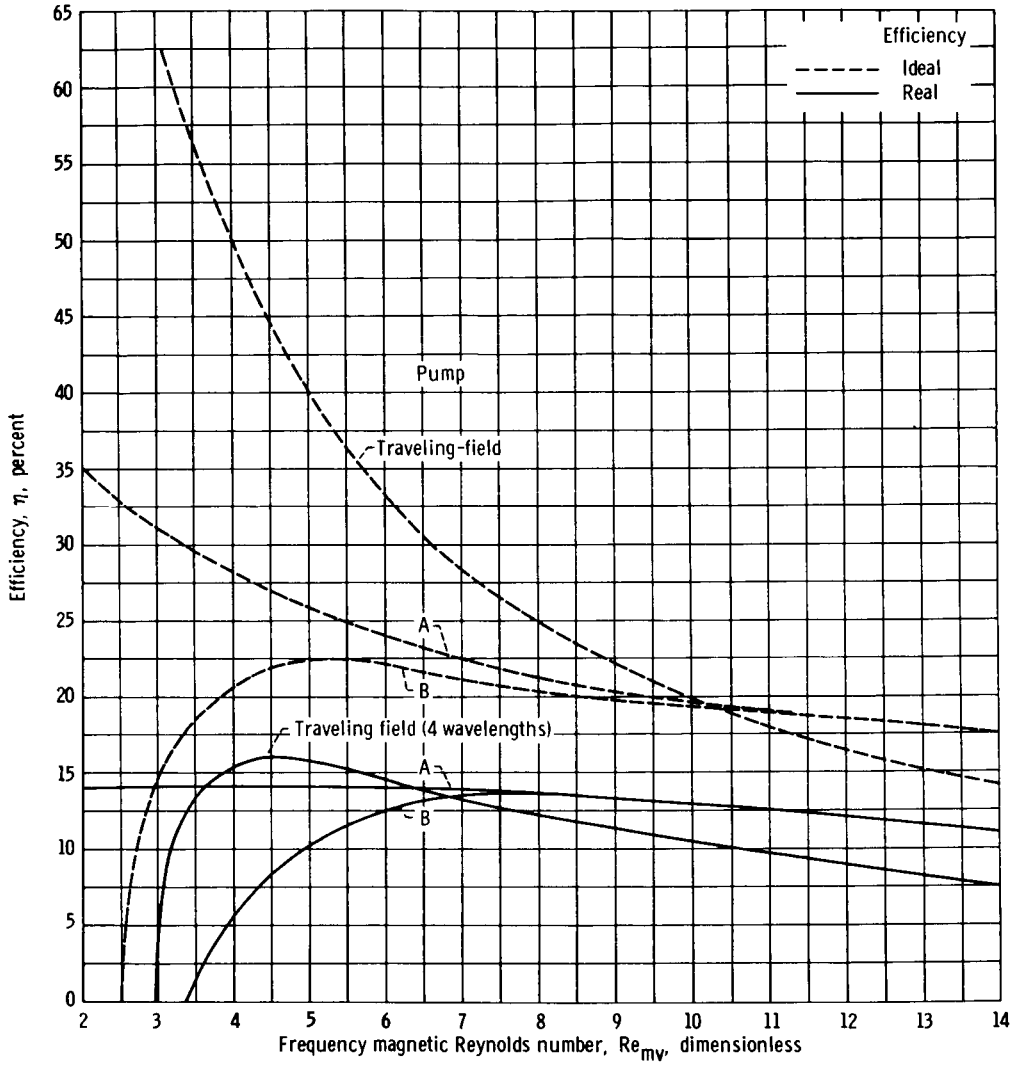

Figure 10. - Overall and ideal efficiencies of single-phase (pumps A and B) and traveling-field electromagnetic pumps. Fluid, lithium; temperature, 922° K (1200° F); flow rate, 10^{-2} cubic meters per second (158 gal/min); output pressure, 10^5 newtons per square meter (14.5 psi); flow magnetic Reynolds number, 2.

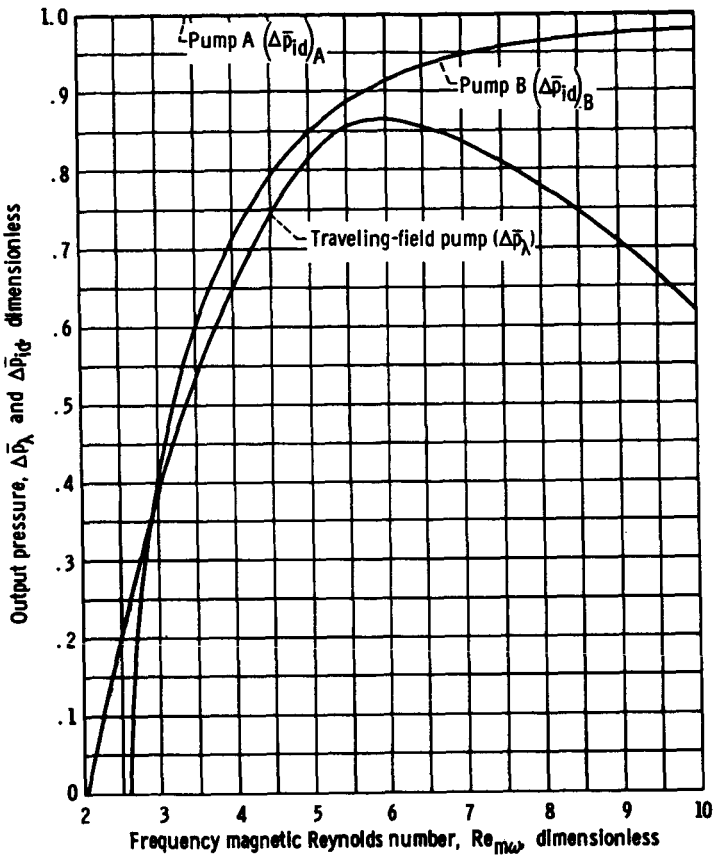

Figure 11. - Dimensionless output pressure of single-phase and traveling-field electromagnetic pumps. Fluid, lithium; temperature, 922° K (1200° F); flow rate, 10^{-2} cubic meters per second (158 gal/min); output pressure, 10^5 newtons per square meter (14.5 psi); flow magnetic Reynolds number, 2.

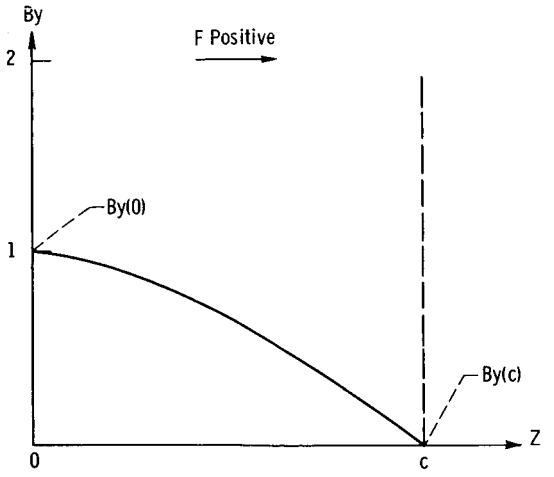

(a) Magnetic field strength as function of axial distance.

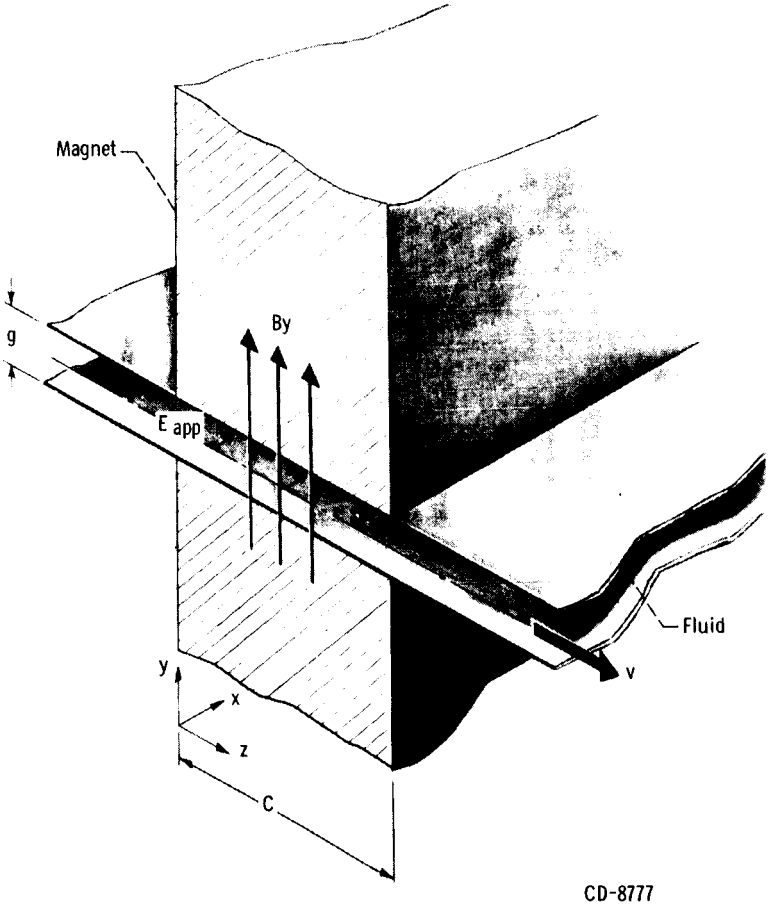

(b) Magnet-fluid geometry.

Figure 12. - Relation of magnetic field distribution to electromagnetic body force (with electric field).

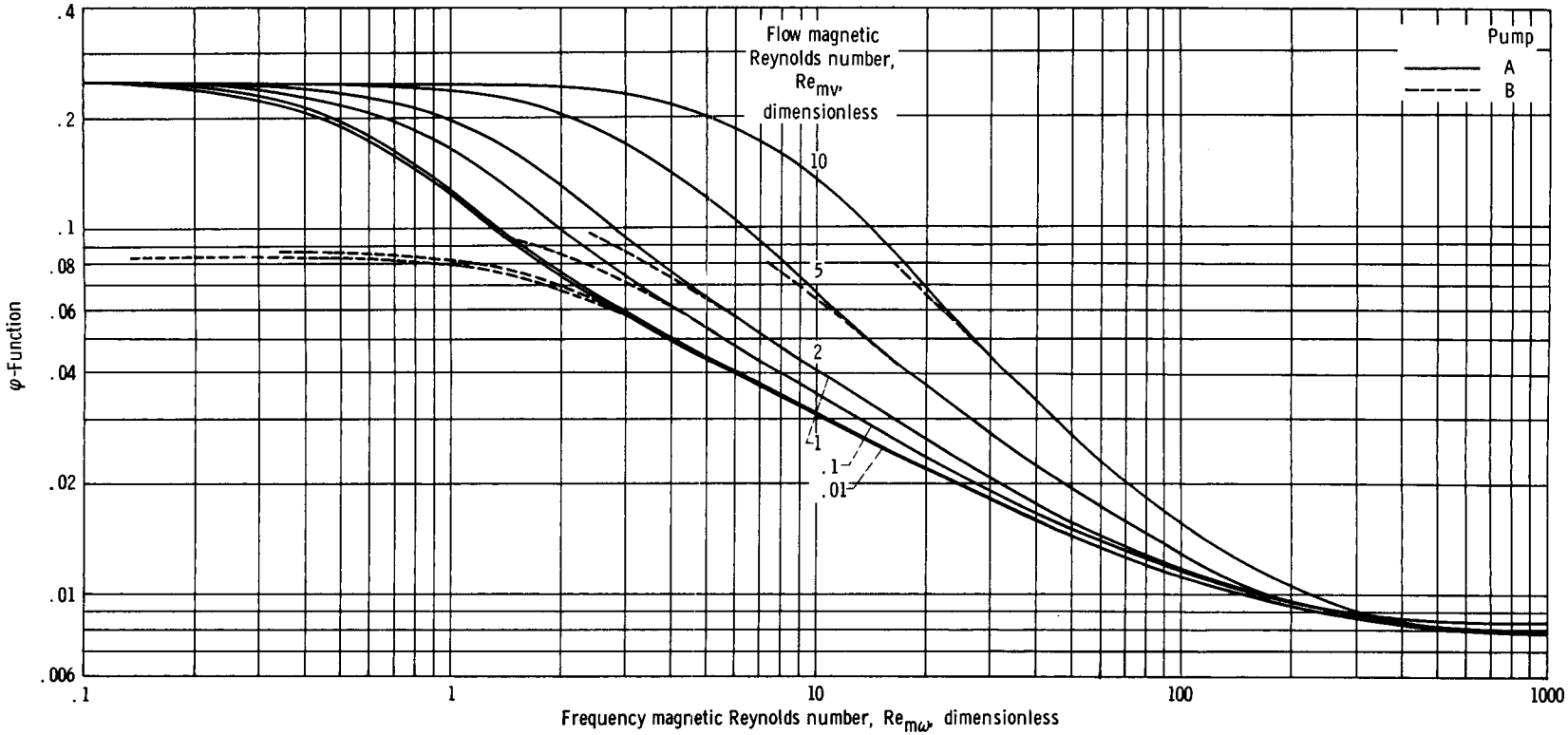

Figure 13. - φ-Function for single-phase induction pumps of zero magnetic field and zero electric field outlet (pumps A and B).

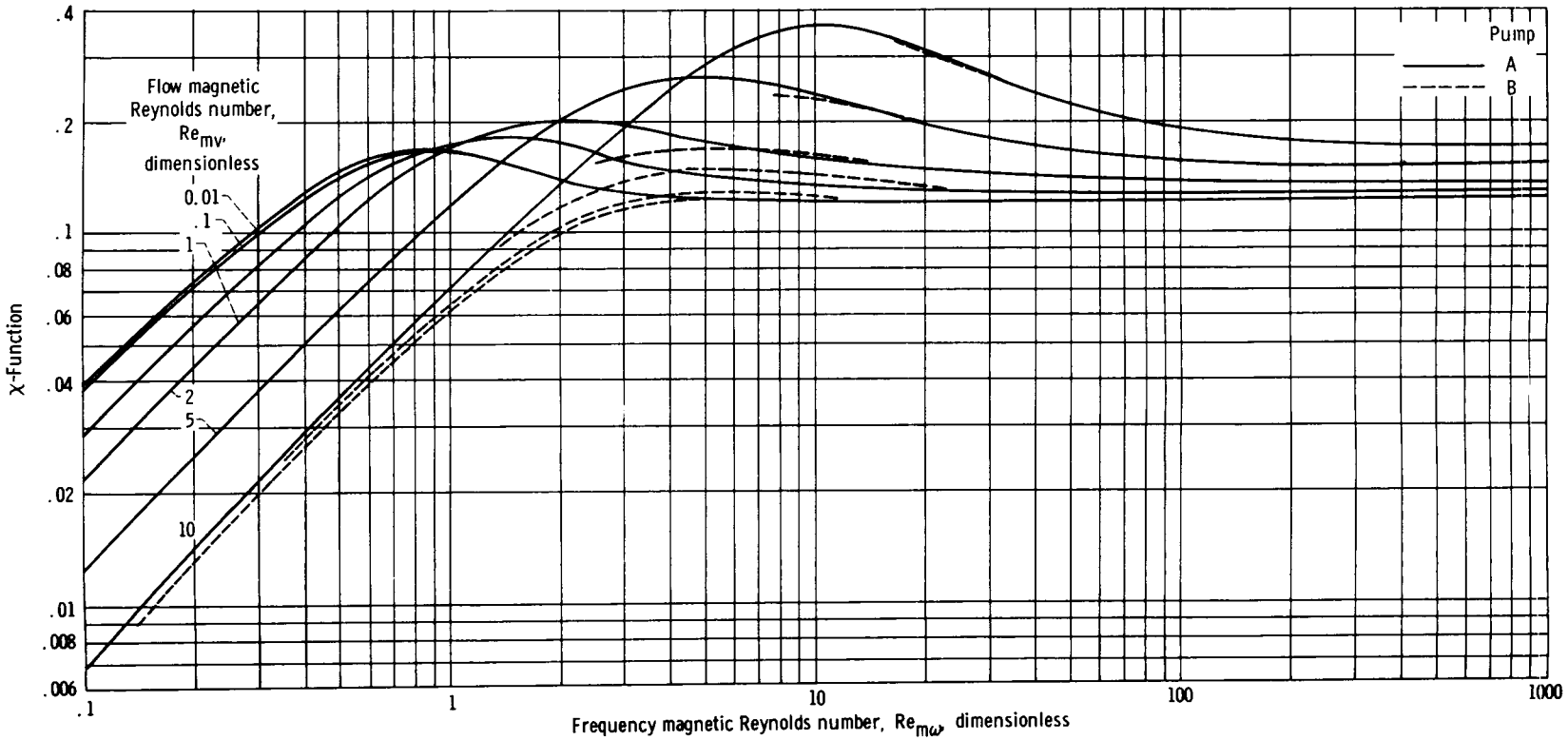

Figure 14. - χ-Function for single-phase induction pumps of zero magnetic field and zero electric field outlet (pumps A and B).

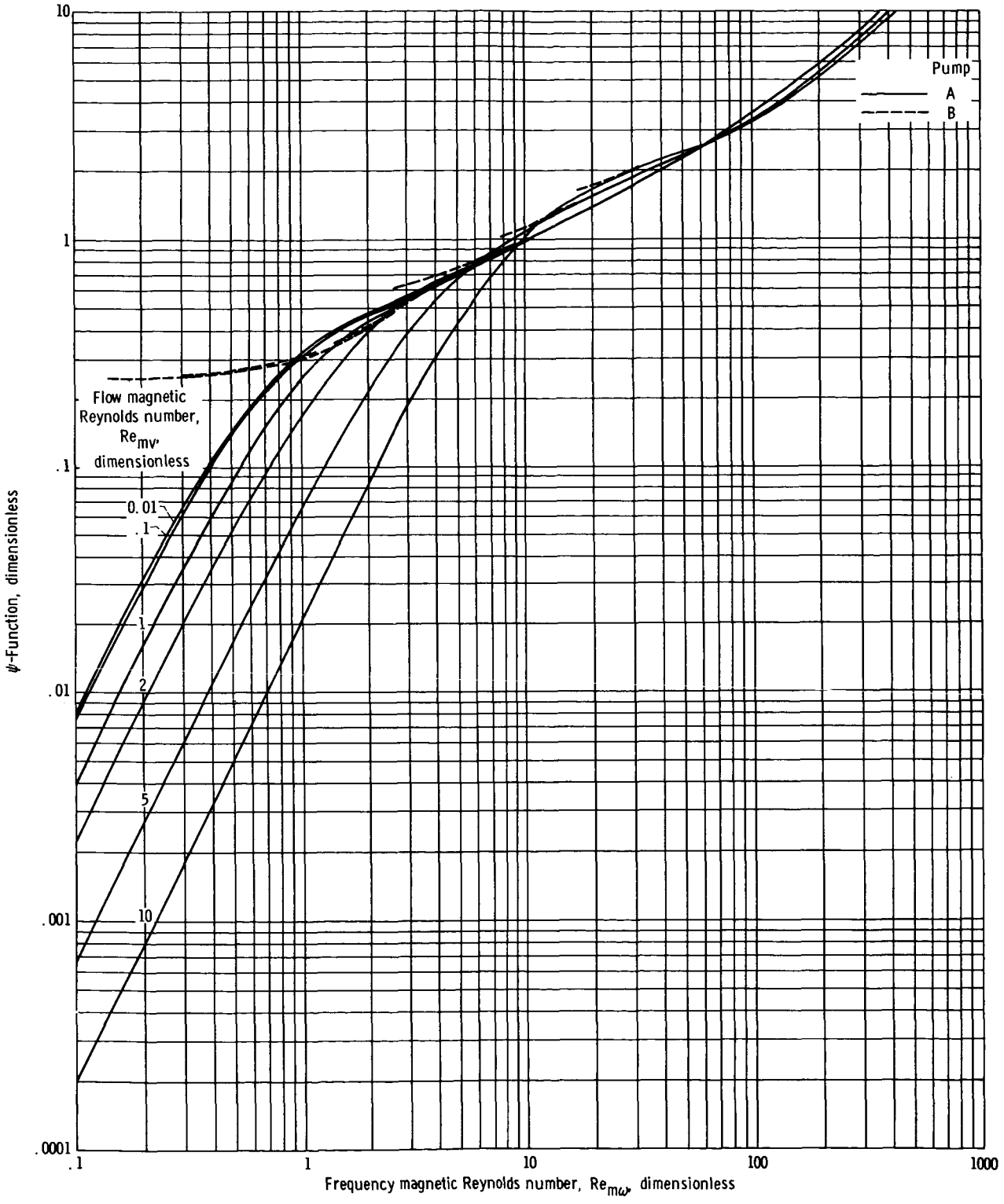

Figure 15. - ψ-Function for single-phase induction pumps A and B with zero magnetic field and zero electric field outlet.

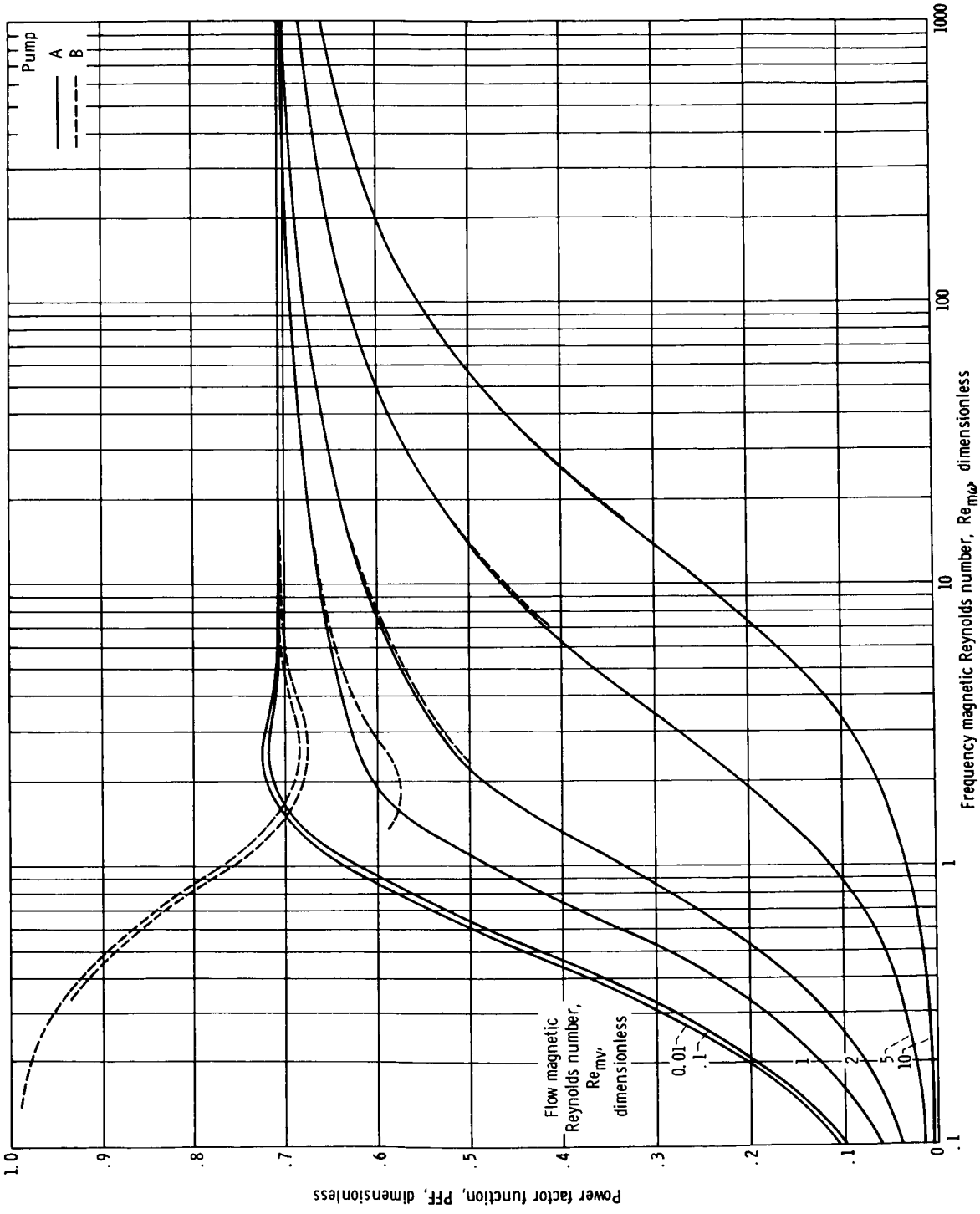

Figure 16. - Power-factor function for single-phase induction pumps A and B with zero magnetic field and zero electric field outlet.

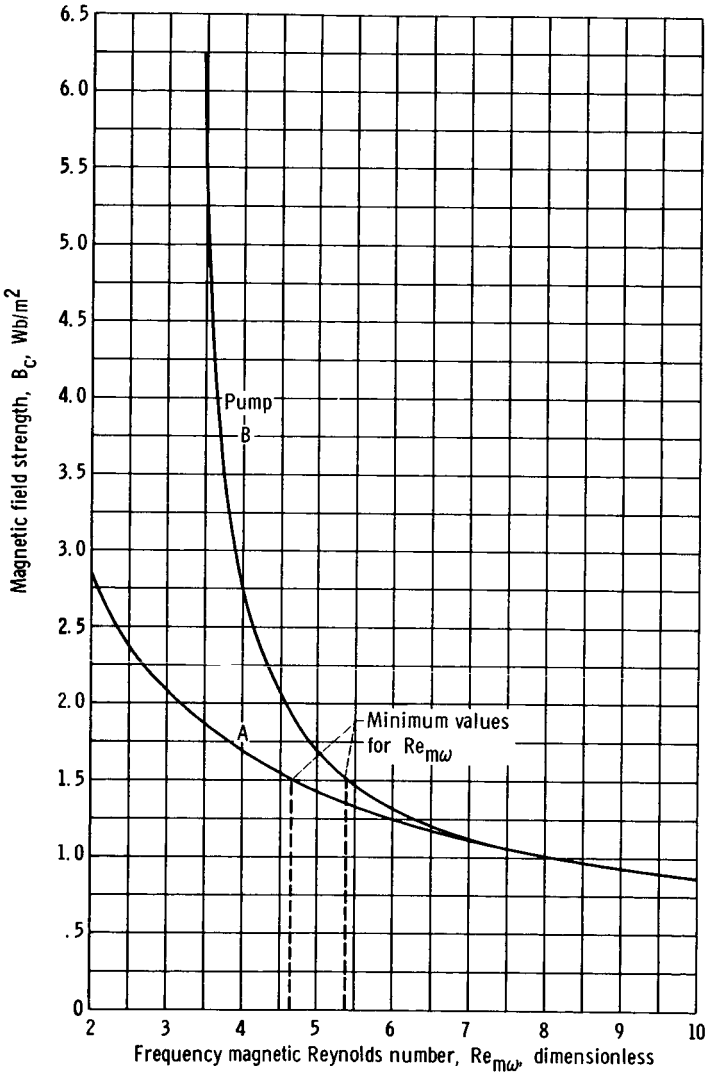

Figure 17. - Required core magnetic field strength of single-phase electromagnetic pumps A and B. Fluid, lithium; temperature, 922° K (1200° F); flow rate, 10^{-2} cubic meters per second (158 gal/min); output pressure, 10^5 newtons per square meter (14.5 psi); flow magnetic Reynolds number, 2.

7/2/67

"The aeronautical and space activities of the United States shall be conducted so as to contribute . . . to the expansion of human knowledge of phenomena in the atmosphere and space. The Administration shall provide for the widest practicable and appropriate dissemination of information concerning its activities and the results thereof."

—NATIONAL AERONAUTICS AND SPACE ACT OF 1958

NASA SCIENTIFIC AND TECHNICAL PUBLICATIONS

TECHNICAL REPORTS: Scientific and technical information considered important, complete, and a lasting contribution to existing knowledge.

TECHNICAL NOTES: Information less broad in scope but nevertheless of importance as a contribution to existing knowledge.

TECHNICAL MEMORANDUMS: Information receiving limited distribution because of preliminary data, security classification, or other reasons.

CONTRACTOR REPORTS: Scientific and technical information generated under a NASA contract or grant and considered an important contribution to existing knowledge.

TECHNICAL TRANSLATIONS: Information published in a foreign language considered to merit NASA distribution in English.

SPECIAL PUBLICATIONS: Information derived from or of value to NASA activities. Publications include conference proceedings, monographs, data compilations, handbooks, sourcebooks, and special bibliographies.

TECHNOLOGY UTILIZATION PUBLICATIONS: Information on technology used by NASA that may be of particular interest in commercial and other non-aerospace applications. Publications include Tech Briefs, Technology Utilization Reports and Notes, and Technology Surveys.

Details on the availability of these publications may be obtained from:

SCIENTIFIC AND TECHNICAL INFORMATION DIVISION

NATIONAL AERONAUTICS AND SPACE ADMINISTRATION

Washington, D.C. 20546